Inorg. Chem. **2004**, *43*, 7709–7725

Homoleptic Cobalt and Copper Phenolate $A_2[M(OAr)_4]$ Compounds: The Effect of Phenoxide Fluorination

Marisa C. Buzzeo,[†] Amber H. Iqbal,[†] Charli M. Long,[†] David Millar,[†] Sonal Patel,[†] Matthew A. Pellow,[†] Sahar A. Saddoughi,[†] Abigail L. Smenton,[†] John F. C. Turner,[‡] Jay D. Wadhawan,[§] Richard G. Compton,[§] James A. Golen,[||,⊥] Arnold L. Rheingold,[||] and Linda H. Doerrer*,[†]

Chemistry Department, Barnard College, 3009 Broadway, New York, New York 10027, Department of Chemistry, University of Tennessee, 409 Buehler Hall, Knoxville, Tennessee 37996, Physical and Theoretical Chemistry Laboratory, University of Oxford, South Parks Road, Oxford, OX1 3QZ, U.K., Department of Chemistry and Biochemistry, University of California—San Diego, 9500 Gilman Drive, MC 0358, La Jolla, California 92093, and Department of Chemistry and Biochemistry, University of Massachusetts—Dartmouth, North Dartmouth, Massachusetts 02747

Received May 8, 2004

Two series of homoleptic phenolate complexes with fluorinated aryloxide ligands $A_2[M(OAr)_4]$ with M = Co^{2+} or Cu^{2+}, $OAr^- = (OC_6F_5)^-$ (OAr^F) or $\{3,5\text{-}OC_6H_3(CF_3)_2\}^-$ (OAr′), A^+ = K (18-crown-6)$^+$, Tl^+, Ph_4P^+, Et_3HN^+, or Me_4N^+ have been synthesized. Two related complexes with nonfluorinated phenoxide ligands have been synthesized and studied in comparison to the fluorinated aryloxides demonstrating the dramatic structural changes effected by modification of OPh to OAr^F. The compounds $\{K(18\text{-crown-6})\}_2[Cu(OAr^F)_4]$, **1a**; $\{K(18\text{-crown-6})\}_2[Cu(OAr')_4]$, **1b**; $[Tl_2Cu(OAr^F)_4]$, **2a**; $[Tl_2Cu(OAr')_4]$, **2b**; $(Ph_4P)_2[Cu(OAr^F)_4]$, **3**; $(^nBu_4N)_2[Cu(OAr^F)_4]$, **4**; $(HEt_3N)_2[Cu(OAr^F)_4]$, **5**; $\{K(18\text{-crown-6})\}_2[Cu_2(\mu_2\text{-}OC_6H_5)_2(OC_6H_5)_4]$, **6**; $\{K(18\text{-crown-6})\}_2[Co(OAr^F)_4]$, **7a**; $\{K(18\text{-crown-6})\}_2[Co(OAr')_4]$, **7b**; $[Tl_2Co(OAr^F)_4]$, **8a**; $[Tl_2Co(OAr')_4]$, **8b**; $(Me_4N)_2[Co(OAr^F)_4]$, **9**; $[Cp_2Co]_2[Co(OAr')_4]$, **10**; and $\{K(18\text{-crown-6})\}_2$-$[Co_2(\mu_2\text{-}OC_6H_5)_2(OC_6H_5)_4]$, **11**, have been characterized with UV–vis and multinuclear NMR spectroscopy and solution magnetic moment studies. Cyclic voltammetry was used to study **1a**, **1b**, **7a**, and **7b**. X-ray crystallography was used to characterize **1b**, **3, 4**, **5**, **6, 7a**, **7b**, **10**, and **11**. The related $[MX_4]^{2-}$ compound $(Ph_4P)_2[Co(OAr^F)_2Cl_2]$, **12**, has also been synthesized and characterized spectroscopically, as well as with conductivity and single-crystal X-ray diffraction. Use of fluorinated aryloxides permits synthesis and isolation of the mononuclear, homoleptic phenolate anions in good yield without oligomerized side products. The reaction conditions that result in homoleptic **1a** and **7a** with OAr^F upon changing the ligand to OPh result in μ_2-OPh bridging phenoxides and the dimeric complexes **6** and **11**. The $[M(OAr^F)_4]^{2-}$ and $[M(OAr')_4]^{2-}$ anions in **1a**, **1b**, **3**, **4**, **5**, **7a**, **7b**, **9**, and **10** demonstrate that stable, isolable homoleptic phenolate anions do not need to be coordinatively or sterically saturated and can be achieved by increasing the electronegativity of the ligand.

Introduction

Homoleptic transition-metal complexes have been an important part of the inorganic chemical literature since Werner's characterization[1] of $[Co(NH_3)_6]^{3+}$. Such compounds often provide archetypal examples of structural and electronic motifs that are more easily understood because of the compositional simplicity of the coordination sphere (e.g., ferrocene,[2] carbonyls,[3] dithiolates,[4] 2,2′-bipyridyl,[5] and hydrides[6]). Not all monodentate ligands stabilize metals equally

* Author to whom correspondence should be addressed. E-mail: ldoerrer@barnard.edu.
[†] Barnard College.
[‡] University of Tennessee.
[§] University of Oxford.
[||] University of California—San Diego.
[⊥] University of Massachusetts—Dartmouth.

(1) Kauffman, G. B. *J. Chem. Educ.* **1966**, *43*, 155−156.
(2) Wilkinson, G.; Rosenblum, M.; Whiting, M. C.; Woodward, R. B. *J. Am. Chem. Soc.* **1952**, *74*, 2125−2126.
(3) Lupinetti, A. J.; Strauss, S. H.; Frenking, G. *Prog. Inorg. Chem.* **2001**, *49*, 1−112.
(4) Stiefel, E. I.; Eisenberg, R.; Rosenberg, R. C.; Gray, H. B. *J. Am. Chem. Soc.* **1966**, *88*, 2956−2966.
(5) Constable, E. C. *Adv. Inorg. Chem.* **1989**, *34*, 1−63.

10.1021/ic0493954 CCC: $27.50
Published on Web 10/29/2004

well, and some have proven quite challenging to impose on transition metals such as methyl groups in homoleptic alkyl compounds.[7−9] Phenoxide and aryloxide groups have been resistive also to preparation as homoleptic derivatives.[10,11] Compounds that contain a subset of aryloxide ligands are legion, owing to interest in these ligands as metal−oxide precursors,[12,13] ancilliary ligands in catalysis,[14−16] and models for metal−tyrosine interactions in biology.[17−20] Much work has demonstrated the tendency of the phenoxide oxygen to bridge metal centers, forming oligomers and polymers that resist purification and characterization.[10]

Inclusion of the phenoxide group in a chelate ring, such as salen-[21] or calixarene-based[22] ligands is the most common approach to forming mononuclear species. Early transition metals in their highest oxidation state with no ligand-field stabliziation energies favor a coordinatively saturated metal center, such as the W^{6+} center in $[W(OC_6H_4\text{-}p\text{-}Me)_6]$.[23] In the early studies of homoleptic alkoxides, this "preference" for coordinative saturation of metal centers was observed to have predictive value in structural determination.[24] Bridging phenoxides also have been avoided by introducing steric bulk in the 2,6 positions on the phenyl ring, preventing close contact of the oxygen atom with more than one metal center.[15,25] Examples of this can be found in the s,[26] p,[27,28] d,[29,30] and f[31] blocks of the periodic table. More recently, fluorinated aryloxides have been investigated, and a few sterically saturated, homoleptic species have been reported for Al^{3+}, Nb^{5+}, and Ta^{5+}. These $[M(OAr)_n]^-$ anions are coordinatively saturated at the metal center and were prepared as possible weakly coordinating anions (WCAs) for use in olefin polymerization catalysis,[32,33] but it was observed that highly electrophilic metal centers (i.e., $[Cp_2ZrMe]^+$) could interact strongly enough with the fluorine atoms in the anions to reduce requisite olefin binding.

Previously, late metal examples of homoleptic alkoxide or aryloxide anions analogous to the well-known anions $[MX_4]^{2-}$, X = halogen or pseudohalogen, were not well-known, and their conspicuous paucity was noted in the literature.[11] Herein we report a detailed and thorough structural study of two families of homoleptic phenolate anions, $[Co(OAr)_4]^{2-}$ and $[Cu(OAr)_4]^{2-}$, that use neither a chelate ring nor steric encumbrance to prevent oligomerization and yet are not coordinatively saturated at the metal center.

Experimental Section

General Information. All studies were carried out at room temperature on a Schlenk line or in a nitrogen- or argon-filled glovebox. For solvents dried in stills, CH_2Cl_2 and CD_2Cl_2 were refluxed over CaH_2. Tetrahydrofuran (THF) and hexane were refluxed over potassium. CH_3CN was predried over P_2O_5 and distilled from CaH_2. Toluene was refluxed over sodium, and ether was refluxed over NaK_3. All solvents were refluxed under nitrogen or argon. Some work also was done with solvents (hexanes, CH_2Cl_2, and toluene) dried in a nitrogen-filled MBraun solvent purification system using Al_2O_3. Celite was dried overnight in vacuo while heated to 125 °C with an oil bath. $KOC_6H_3(CF_3)_2$ (KOAr′) and KOC_6H_5 (KOPh) were prepared according to our previously published procedure.[34] $\{^nBu_4N\}_2[CuCl_4]$ was prepared by the literature procedure.[35] 18-crown-6 was recrystallized from either hexanes or CH_3CN. All other reagents were obtained commercially and were not purified further. NMR spectra were measured on a Varian 300-MHz, Bruker 300- or 400-MHz spectrometer. ^1H and ^{13}C chemical shifts were referenced to $(CH_3)_4Si$ via the resonance of residual protiosolvent (^1H) or the ^{13}C resonance of the solvent. ^{19}F shifts were referenced to external $CFCl_3$. UV−vis data were recorded with a Varian Cary 50 spectrometer. IR spectra were recorded on a Perkin-Elmer Spectrum BX instrument with Nujol mulls between NaCl plates. Solution phase magnetic susceptibilities were determined by Evans' method[36,37] in d_6-acetone with 10% $(Me_3Si)_2O$ and the same solution as an internal reference and are reported after correction using appropriate diamagnetic terms.[38,39] Microanalyses were preformed by H. Kolbe Microanalytisches Laboratorium, Mülheim an der Ruhr, Germany.

Synthetic Procedures. K(OAr^F). This compound has been reported previously in the literature as a reagent,[40−44] but we are

(6) King, R. B. *Coord. Chem. Rev.* **2000**, *200−202*, 813−829.
(7) LaPointe, A. M. *Inorg. Chim. Acta* **2003**, *345*, 359−362.
(8) Schulzke, C.; Enright, D.; Sugiyama, H.; LeBlanc, G.; Gambarotta, S.; Yap, G. P. A.; Thompson, L. K.; Wilson, D. R.; Duchateau, R., *Organometallics* **2002**, *21*, 3810−3816.
(9) Wilkinson, G. *Sci. Prog.* **1994**, *77*, 15−27.
(10) Bradley, D. C.; Mehrotra, R. C.; Rothwell, I. P.; Singh, A. *Alkoxo and Aryloxo Derivatives of Metals*; Academic Press: New York, 2001.
(11) Cotton, F. A.; Liu, C. Y.; Murillo, C. A.; Wang, X. *Inorg. Chem.* **2003**, *42*, 4619−4623.
(12) Henderson, K. W.; Mulvey, R. E.; Reinhard, F. B. M.; Clegg, W.; Horsburgh, L. *J. Am. Chem. Soc.* **1994**, *116*, 10777−10778.
(13) Boyle, T. J.; Pedrotty, D. M.; Alam, T. M.; Vick, S. C.; Rodriguez, M. A. *Inorg. Chem.* **2000**, *39*, 5133−5146.
(14) Churchill, M. R.; Ziller, J. W.; Freudenberger, J. H.; Schrock, R. R. *Organometallics* **1984**, *3*, 1554−1562.
(15) Rothwell, I. P. *Chem. Commun.* **1997**, 1331−1338.
(16) Darensbourg, D. J.; Wildeson, J. R.; Yarbrough, J. C.; Reibenspies, J. H. *J. Am. Chem. Soc.* **2000**, *122*, 12487−12496.
(17) Koch, S. A.; Millar, M. *J. Am. Chem. Soc.* **1982**, *104*, 5255−5257.
(18) Kim, E.; Chufan, E. E.; Kamaraj, K.; Karlin, K. D. *Chem. Rev.* **2004**, *104*, 1077−1133.
(19) Lewis, E. A.; Tolman, W. B. *Chem. Rev.* **2004**, *104*, 1047−1076.
(20) Mirica, L. M.; Ottenwaelder, X.; Stack, T. D. P. *Chem. Rev.* **2004**, *104*, 1013−1045.
(21) Jacobsen, E. N. *Acc. Chem. Res.* **2000**, *33*, 421−431.
(22) Roundhill, D. M. *Prog. Inorg. Chem.* **1995**, *43*, 533−592.
(23) Clegg, W.; Errington, R. J.; Kraxner, P.; Redshaw, C. *J. Chem. Soc., Dalton Trans.* **1992**, 1431−1438.
(24) Bradley, D. C.; Mehrotra, R. C.; Rothwell, I. P.; Singh, A. In *Alkoxo and Aryloxo Derivatives of Metals*; Academic Press: New York, 2001; Chapter 2, p 3.
(25) Gardiner, I. M.; Bruck, M. A.; Wexler, P. A.; Wigley, D. E. *Inorg. Chem.* **1989**, *28*, 3688−3695.
(26) Bell, N. A.; Coates, G. E.; Shearer, H. M. M.; Twiss, J. *J. Chem. Soc., Chem. Commun.* **1983**, 840−841.
(27) Cetinkaya, B.; Gumrukcu, I.; Lappert, M. F.; Atwood, J. L.; Rogers, R. D.; Zaworotko, M. J. *J. Am. Chem. Soc.* **1980**, *102*, 2088−2089.
(28) Hitchcock, P. B.; Lappert, M. F.; Thomas, S. A.; Thorne, A. J.; Carty, A. J.; Taylor, N. J. *J. Organomet. Chem.* **1986**, *315*, 27−44.
(29) Meyer, D.; Osborn, J. A.; Wesolek, M. *Polyhedron* **1990**, *9*, 1311−1315.
(30) Darensbourg, D. J.; Wildeson, J. R.; Lewis, S. J.; Yarbrough, J. C. *J. Am. Chem. Soc.* **2002**, *124*, 7075−7083.
(31) McKee, S. D.; Burns, C. J.; Avens, L. R. *Inorg. Chem.* **1998**, *37*, 4040−4045.
(32) Sun, Y.; Metz, M. V.; Stern, C. L.; Marks, T. J. *Organometallics* **2000**, *19*, 1625−1627.
(33) Metz, M. V.; Sun, Y.; Stern, C. L.; Marks, T. J. *Organometallics* **2002**, *21*, 3091−3102.
(34) Buzzeo, M. C.; Zakharov, L. N.; Rheingold, A. L.; Doerrer, L. H. *J. Mol. Struct.* **2003**, *657*, 19−24.
(35) Gill, N. S.; Taylor, F. B. *Inorg. Synth.* **1967**, *9*, 136−142.
(36) Evans, D. F. *J. Chem. Soc.* **1959**, 2003−2005.
(37) Sur, S. K. *J. Magn. Reson.* **1989**, *82*, 169−173.
(38) O'Connor, J. C. *Prog. Inorg. Chem.* **1982**, *29*, 203−283.
(39) Kahn, O. *Molecular Magnetism*; VCH: New York, 1993.
(40) Pasenok, S. V.; Yagupolskii, Y. L.; Tyrra, W.; Naumann, D. *Z. Anorg. Allg. Chem.* **1999**, *625*, 831−833.

not aware of any characterization data and therefore present the synthesis and spectroscopy here. A portion of $HOAr^F$ (6.85 g, 37.4 mmol) was dissolved in 20 mL of THF to which a slurry of KH (1.5 g, 37.4 mmol) in 20 mL of THF was added slowly over several minutes with vigorous stirring. The solution was allowed to stir for 45 min, and the THF was removed in vacuo. The crude material was recrystallized from THF and pentanes. Recrystallized yield: 7.5 g (90%). $^{13}C\{^1H\}$ NMR (δ, ppm $\{(CD_3)_2CO\}$): 127.5 (*p*, d, $^1J_{CF} = 228.5$ Hz), 139.63 (*m*, d, $^1J_{CF} = 245.8$ Hz), 142.32 (*o*, d, $^1J_{CF} = 229.0$ Hz), 147.7 (*i*, d, $^2J_{CF} = 13.2$ Hz). ^{19}F NMR (δ, ppm, $\{(CD_3)_2CO\}$): −173.6 (*o*-F, *m*-F, multiplet), −193.9 (*p*-F, t, $^3J_{FF} = 18.3$ Hz).

Tl(OAr^F). This compound also previously has been reported in the literature[45−50] as a reagent, and we report the synthesis and spectroscopic data that characterize this material here for the same reasons as for $K(OAr^F)$. A 25-g portion of TlOEt (100.23 mmol) was added via syringe to 18.45 g of $HOAr^F$ (100.23 mmol) in 500 mL of CH_2Cl_2 with vigorous stirring. The reaction was allowed to stir for 5 h after which time a large amount of white precipitate had formed. The supernatant was pale purple-brown and was decanted. The product was washed four times with ∼125 mL portions of hexane and dried in vacuo. Yield: 33.9 g (87.4%). $^{13}C\{^1H\}$ NMR (δ, ppm, $\{(CD_3)_2CO\}$): 131.77 (*p*, d, $^1J_{CF} = 239.4$ Hz), 139.37 (*ipso*, s), 139.53 (*m*, d, $^1J_{CF} = 239.4$ Hz), 142.39 (*o*, d, $^1J_{CF} = 233.0$ Hz). ^{19}F NMR (δ, ppm, $\{(CD_3)_2CO\}$): −159.73 (*p*-F, s), −165.57 (*m*-F, t, $^3J_{FF} = 21.2$ Hz), −176.88 (*o*-F, m).

Tl(OAr′). A procedure similar to that for $Tl(OAr^F)$ was followed. A 19.73-g portion of TlOEt (79 mmol) was added via syringe to 19.11 g of HOAr′ (83 mmol) in 100 mL of toluene with vigorous stirring. The reaction was allowed to stir overnight after which time a large amount of white precipitate had formed. Toluene and ethanol were removed in vacuo, and the product was redissolved in warm toluene, filtered, and upon cooling layered with room-temperature hexanes. Yield: 25.6 g (74.7%). ^1H NMR (δ, ppm, $\{(CD_3)_2CO\}$): 7.004 (*p*, 1H), 7.288 (*o*, 2H). $^{13}C\{^1H\}$ NMR (δ, ppm, $\{(CD_3)_2CO\}$): 107.42 (*p*, septet, $^3J_{CF} = 4.1$ Hz), 119.86 (*o*, s), 132.69 (*m*, q, $^2J_{CF} = 31.78$ Hz), 125.31 (*C*F_3, q, $^1J_{CF} = 271.9$ Hz), 168.17 (*ipso*, s). ^{19}F NMR (δ, ppm, $\{(CD_3)_2CO\}$): −62.20 (C*F*$_3$, s).

{K(18-crown-6)}$_2$[Cu(OAr^F)$_4$], 1a. A portion of $KOAr^F$ (357 mg, 1.609 mmol) was dissolved in 4 mL of THF and then added to an orange-brown slurry of (89.8 mg, 0.402 mmol) $CuBr_2$ in 4 mL of THF causing immediate formation of a dark green mixture. The solution was stirred at room temperature overnight after which time the solution was concentrated to dryness and triturated three times with 5 mL of hexanes. A 2-equiv portion of 18-crown-6 (212.6 mg, 0.804 mmol) and 8 mL of CH_2Cl_2 were added. After 30 min, the deep-green solution was separated from a white precipitate, presumed to be KBr, via filtration through Celite and concentrated to dryness in vacuo, and the crude product was recrystallized from CH_2Cl_2 and pentanes. The product was isolated in 53% recrystallized yield (300 mg). ^1H NMR (δ, ppm, $\{(CD_3)_2CO\}$): 3.64 (s, 48H, C*H*$_2$). $^{13}C\{^1H\}$ NMR (δ, ppm, $\{(CD_3)_2CO\}$): 70.97 (s, *C*H$_2$). UV−vis (THF) (λ_{max}, nm (ϵ_M, cm^{-1} M^{-1})): 265 (3900), 329 (1800), 422 (1010). Anal. Calcd for $C_{48}H_{48}O_{16}F_{20}K_2Cu$: C, 41.10; H, 3.45. Found: C, 41.18; H, 3.50. μ_{eff} (Evans' method) = 1.74μ_B.

{K(18-crown-6)}$_2$[Cu(OAr′)$_4$], 1b. A portion of KOAr′ (350.0 mg, 1.305 mmol) was dissolved in 4 mL of THF and then added to $CuBr_2$ (72.9 mg, 0.326 mmol) following the same procedure as for **1a**, including the addition of 2 equiv of 18-crown-6 (172.5 mg, 0.653 mmol). The crude product was recrystallized from CH_2Cl_2 and pentanes in 48% yield (248 mg). X-ray quality crystals were grown from the same solvent mixture. ^1H NMR (δ, ppm, $\{(CD_3)_2CO\}$): 3.72 (s, 48H, C*H*$_2$). $^{13}C\{^1H\}$ NMR (δ, ppm, $\{(CD_3)_2CO\}$): 71.02 (s, *C*H$_2$). UV−vis (THF) (λ_{max}, nm (ϵ_M, cm^{-1} M^{-1})) 308 (7810), 360 (sh) (1659). Anal. Calcd for $C_{56}H_{60}O_{16}F_{24}K_2Cu$: C, 42.39; H, 3.81. Found: C, 42.35; H, 3.89. μ_{eff} (Evans' method) = 1.79μ_B.

[Tl$_2$Cu(OAr^F)$_4$], 2a. A portion of $CuBr_2$ (72.1 mg, 0.3226 mmol) was dissolved in 6 mL of THF to give an orange-brown solution. A 3-mL solution of 4 equiv of $TlOAr^F$ (500.0 mg, 1.291 mmol) was added to the first solution causing instant precipitation of a white solid, assumed to be TlBr. The solution was allowed to stir overnight, after which time the solid was removed via filtration, and the filtrate was concentrated to ∼2 mL in vacuo. The solution volume was increased to 20 mL with pentane and left at room temperature. Very fine brown needles precipitated overnight. This material was recrystallized twice more from THF/pentane at −40 °C, collected by filtration, and dried in vacuo. Final recrystallized yield 210 mg (54% yield). UV−vis (THF) (λ_{max}, nm (ϵ_M, cm^{-1} M^{-1})) 441 (2450). Anal. Calcd for $C_{24}O_4F_{20}CuTl_2$: C, 23.93, F, 31.54. Found: C, 24.10, F, 31.31. μ_{eff} (Evans' method) = 1.79μ_B.

[Tl$_2$Cu(OAr′)$_4$], 2b. A procedure analogous to that for **2a** was followed with $CuBr_2$ (51.5 mg, 0.2307 mmol) and 4 equiv of $TlOAr^F$ (400.0 mg, 0.9228 mmol). Recrystallization from THF and hexanes gave 278 mg (45.6% yield) of dark brown microcrystalline product. UV−vis (THF) (λ_{max}, nm (ϵ_M, cm^{-1} M^{-1})): 421 (2500). Anal. Calcd for $C_{46}H_{40}O_{7.5}F_{24}CuTl_2$ (**2b**·3.5 THF): C, 33.67; H, 2.46; F, 27.78. Found: C, 33.54; H, 2.41; F, 27.92. μ_{eff} (Evans' method) = 1.94μ_B.

(Ph$_4$P)$_2$[Cu(OAr^F)$_4$], 3. A portion of $CuBr_2$ (223.4 mg, 1.00 mmol) was dissolved in 10 mL of THF, and 4 equiv of $TlOAr^F$ (1.5 g, 4.00 mmol) in a further 10 mL of THF was added. Formation of a precipitate, presumably TlBr, was observed instantly. The solution was stirred overnight and then filtered through Celite to remove the precipitate. To the resulting orange-brown solution, 2 equiv of Ph_4PI (932.6 mg, 2.00 mmol) was added, causing instant formation of a yellow solid, presumed to be TlI, and a solution color change to deep green. The solution was allowed to stir for 2 h and filtered again through Celite, and the filtrate was concentrated to dryness in vacuo. The crude powder was recrystallized three times from CH_2Cl_2/pentane mixtures. Yield: 1.07 g (73%). ^1H NMR (δ, ppm, $\{(CD_3)_2CO\}$): 7.838 (br), 8.018 (br). $^{13}C\{^1H\}$ NMR (δ, ppm, $\{(CD_3)_2CO\}$): 119.15 (*ipso*, d, $^1J_{C-P} = 89.6$ Hz), 131.51 (*o*, d, $^2J_{C-P} = 12.7$ Hz), 135.83 (*m*, d, $^3J_{C-P} = 10.1$ Hz), 136.49 (s, para). UV−vis (THF) (λ_{max}, nm (ϵ_M, cm^{-1} M^{-1})): 330 (sh) (5470),

(41) Seidel, S. W.; Schrock, R. R.; Davis, W. M. *Organometallics* **1998**, *17*, 1058−1068.
(42) Schofield, M. H.; Schrock, R. R.; Park, L. Y. *Organometallics* **1991**, *10*, 1844−1851.
(43) Schrock, R. R.; Kolodziej, R. M.; Liu, A. H.; Davis, W. M.; Vale, M. G. *J. Am. Chem. Soc.* **1990**, *112*, 4338−4345.
(44) Liu, A. H.; Murray, R. C.; Dewan, J. C.; Santarsiero, B. D.; Schrock, R. R. *J. Am. Chem. Soc.* **1987**, *109*, 4282−4291.
(45) Zanella, P.; Mascellani, N.; Cason, A.; Garon, S.; Rossetto, G.; Carta, G. *Appl. Organomet. Chem.* **2001**, *15*, 717−724.
(46) Curnow, O. J.; Hughes, R. P. *J. Am. Chem. Soc.* **1992**, *114*, 5895−5897.
(47) Danopoulos, A. A.; Wilkinson, G.; Sweet, T. K. N.; Hursthouse, M. B. *Polyhedron* **1994**, *13*, 2899−2905.
(48) Danopoulos, A. A.; Wilkinson, G.; Sweet, T. K. N.; Hursthouse, M. B. *J. Chem. Soc., Dalton Trans.* **1994**, 1037−1049.
(49) Hughes, R. P.; Zheng, X.; Ostrander, R. L.; Rheingold, A. L. *Organometallics* **1994**, *13*, 1567−1568.
(50) Davidson, J. L.; Holz, B.; Leverd, P. C.; Lindsell, W. E.; Simpson, N. J. *J. Chem. Soc., Dalton Trans.* **1994**, 3527−3532.

411 (3630). Anal. Calcd for $C_{72}H_{40}O_4F_{20}CuP_2$: C, 58.65; H, 2.73. Found: C, 58.63; H, 2.75. μ_{eff} (Evans' method) = 1.69μ_B.

(^{n}Bu$_4$N)$_2$[Cu(OAr^F)$_4$], 4. A portion of (^{n}Bu$_4$N)$_2$[CuCl$_4$] (1.78 g, 0.258 mmol) and 4 equiv of TlOAr^F (4.00 g, 1.03 mmol) were dissolved in toluene resulting in precipitation of presumed TlCl and formation of a green solution. The white precipitate was removed via filtration, and the solution was placed at −80 °C overnight. Green crystals were formed, isolated via filtration, washed with hexanes, and dried under vacuum. Single crystals for X-ray crystallography were grown slowly from THF/pentane mixtures. ^{1}H NMR (δ, ppm, {(CD$_3$)$_2$CO}): 1.034 (b, 3H, C−C*H*$_3$), 1.502 (b, 2H, C*H*$_2$−CH$_3$), 1.753 (b, 2H, C*H*$_2$−CH$_2$−CH$_3$), 3.245 (b, 2H, C*H*$_2$−C−C−C), ^{13}C NMR (δ, ppm, {(CD$_3$)$_2$CO}): 13.359 (C−*C*H$_3$), 19.930 (*C*H$_2$−CH$_3$), 24.055 (*C*H$_2$−CH$_2$−CH$_3$), 59.032 (*C*H$_2$−C−C−C). UV−vis (THF) (λ_{max}, nm (ϵ_M, cm^{-1} M^{-1})): 322 (sh) (4810), 414 (3370). Anal. Calcd for $C_{56}H_{72}N_2O_4F_{20}Cu$: C, 52.52; H, 5.67; N, 2.19. Found: C, 52.61; H, 5.69; N, 2.09. μ_{eff} (Evans' method) = 1.87μ_B.

(HEt$_3$N)$_2$[Cu(OAr^F)$_4$], 5. To a portion of CuCl$_2$·2H$_2$O (830.6 mg, 6.18 mmol) in 25 mL of CH$_2$Cl$_2$, a mixture of 4 equiv of Et$_3$N (3.44 mL, 24.71 mmol) and 4 equiv of HOAr^F (4.549 g, 24.71 mmol) in 25 mL of CH$_2$Cl$_2$ was added. **N.B.** The amine and phenol must react together prior to introduction of Cu^{II} because Et$_3$N readily deprotonates water from CuCl$_2$·2H$_2$O and forms Et$_3$HNCl and the insoluble, bright blue [Cu(OH)$_2$] precipitate. The reaction mixture was allowed to stir overnight and then added to an equal volume of water. The ammonium salts were removed, the organic layer was washed with water twice more, and the combined organic fractions were dried over MgSO$_4$. The desiccant was removed via filtration, and the product was recrystallized from THF and hexanes to give 5.23 g (84.7% yield) of a yellow-green powder. X-ray quality crystals were grown from the same mixture. ^{1}H NMR (δ, ppm, {(CD$_3$)$_2$CO}): 1.386 (br, 12H, C*H*$_3$), 3.006 (br, 8H, C*H*$_2$). ^{13}C{^{1}H} NMR (δ, ppm, {(CD$_3$)$_2$CO}): 9.21 (s, *C*H$_3$), 69.27 (s, *C*H$_2$) UV−vis (THF) (λ_{max}, nm (ϵ_M, cm^{-1} M^{-1})): 264 (9870), 330 (sh) (2380) 432 (1990). Anal. Calcd for $C_{36}H_{32}N_2O_4F_{20}Cu$: C, 43.23; H, 3.22; N, 2.80. Found: C, 43.32; H, 3.16; N, 2.77. μ_{eff} (Evans' method) = 1.72μ_B.

{K(18-crown-6)}$_2$[Cu$_2$(μ_2-OC$_6$H$_5$)$_2$(OC$_6$H$_5$)$_4$], 6. A 1-equiv portion of CuBr$_2$ (1.009 mmol, 225.3 mg) was dissolved in 5 mL of THF to which 3 equiv of KOPh (3.026 mmol, 400.0 mg) in 15 mL of THF was added. The reaction mixture was stirred overnight, then the resulting brown solution was filtered through Celite to remove white (presumed) KBr, and the filtrate was concentrated to dryness in vacuo. After the sample was tritruated three times with 3 mL of CH$_2$Cl$_2$ and 1 equiv of 18-crown-6 (1.009 mmol, 266.6 mg) was added, the solution was filtered again through Celite and concentrated to dryness and the orange-brown product was recrystallized from CH$_2$Cl$_2$ and hexanes to give 160 mg of dark brown microcrystalline material (24.6% yield). X-ray quality crystals were grown from the same mixture. ^{1}H NMR (δ, ppm, {(CD$_3$)$_2$CO}): 3.660 (s, 24H, C*H*$_2$). ^{13}C{^{1}H} NMR (δ, ppm, {(CD$_3$)$_2$CO}): 71.01 (s, *C*H$_2$) UV−vis (THF) (λ_{max}, nm (ϵ_M, cm^{-1} M^{-1})): 281 (13,250), 390 (br) (1370) Anal. Calcd For $C_{60}H_{78}O_{18}K_2Cu_2$: C, 55.75; H, 6.08. Found: C, 55.59; H, 6.15. μ_{eff} (Evans' method) = 2.74μ_B.

{K(18-crown-6)}$_2$[Co(OAr^F)$_4$], 7a. A 1-equiv portion of CoI$_2$ (0.450 mmol, 140.8 mg) and 4 equiv of KOAr^F (1.80 mmol and 400.0 mg) were combined in 20 mL of THF and allowed to stir overnight. The solution turned deep cobalt blue, and white (presumed) KI precipitated. The solid was removed via filtration through Celite, the solvent was removed in vacuo, and the resultant blue powder was triturated 3 times with hexane to give a purple powder. A 2-equiv portion of 18-crown-6 (0.900 mmol, 238.0 mg) was added to 10 mL of CH$_2$Cl$_2$ to give a cobalt blue solution that was filtered through Celite and concentrated to dryness. The crude product was recrystallized from CH$_2$Cl$_2$ layered with hexanes to give crystals that rapidly desolvated upon removal of the supernatant. Complete removal of the solvent yielded 390 mg of blue powder (62% yield). X-ray quality crystals were grown from THF and pentanes. ^{1}H NMR (δ, ppm, {(CD$_3$)$_2$CO}): 3.440 (s, 48H, C*H*$_2$). ^{13}C{^{1}H} NMR (δ, ppm, {(CD$_3$)$_2$CO}): 70.72 (s, *C*H$_2$). UV−vis (THF) (λ_{max}, nm (ϵ_M, cm^{-1} M^{-1})): 532 (110), 598 (220), 651 (260). Anal. Calcd for $C_{48}H_{48}O_{16}F_{20}K_2Co$: C, 41.24; H, 3.46. Found: C, 41.28; H, 3.43. μ_{eff} (Evans' method) = 4.53μ_B.

{K(18-crown-6)}$_2$[Co(OAr′)$_4$], 7b. A portion of CoI$_2$ (0.1896 mmol, 59.3 mg) was dissolved in 5 mL of THF to which was added a solution of 4 equiv of KOAr′ (0.7585 mmol, 208.9 mg) in 5 mL of THF. Subsequent workup was analogous to that of **7a**, including addition of 2 equiv of 18-crown-6 (0.3792 mmol, 100 mg), removal of precipitates, and recrystallization from CH$_2$Cl$_2$ and hexanes to give 161 mg (54.2% yield) of cobalt blue crystalline material. X-ray quality crystals were grown from the same mixture. ^{1}H NMR (δ, ppm, {(CD$_3$)$_2$CO}): 3.674 (s, 48H, C*H*$_2$). ^{13}C{^{1}H} NMR (δ, ppm, {(CD$_3$)$_2$CO}): 70.96 (s, *C*H$_2$). UV−vis (THF) (λ_{max}, nm (ϵ_M, cm^{-1} M^{-1})): 550 (360), 597 (540), 632 (510). Anal. Calcd for $C_{56}H_{60}O_{16}F_{24}K_2Co$: C, 42.51; H, 3.82. Found: C, 42.58; H, 3.87. μ_{eff} (Evans' method) = 5.02μ_B.

[Tl$_2$Co(OAr^F)$_4$], 8a. In the drybox 4 equiv of TlOAr^F (1.292 g, 3.33 mmol) was dissolved in THF and 1 equiv of CoI$_2$ (0.261 g, 0.833 mmol) was added while the solution was stirring. A dark deep blue solution with yellow precipitate was formed. After the solution was stirred overnight, it was filtered through Celite, and the solvent was removed in vacuo. A dark purple solid remained, which was triturated 3 times with 2 mL of hexane. The product was dissolved in a minimum amount of toluene, filtered, and layered with hexane. The mixture was stored at −30 °C, and after 1 day the product was isolated by filtration, leaving a purple colored solid in 73% yield. X-ray quality crystals were grown from toluene and hexanes. UV−vis (toluene) (λ_{max}, nm (ϵ_M, M^{-1} cm^{-1})): 510 (320), 530 (350), 584.9 (530). UV−vis (THF) (λ_{max}, nm (ϵ_M, M^{-1} cm^{-1})): 533 (230), 586 (340). Anal. Calcd for $C_{24}O_4F_{20}CoTl_2$: C, 24.02; F, 31.67. Found: C, 23.86; F, 31.43. μ_{eff} (Evans' method) = 4.46μ_B.

[Tl$_2$Co(OAr′)$_4$], 8b. A 4-equiv portion of Tl(OAr′) (3.763 g, 8.68 mmol) was dissolved in THF, and 1 equiv of CoI$_2$ (0.679 g, 2.17 mmol) was added while stirring. A dark blue solution with yellow precipitate was formed. Workup followed the same procedure as that for **8a**. The resulting purple powder was dissolved in a minimum amount of toluene, filtered, layered with hexane for recrystallization, and left at −30 °C. A purple crystalline solid was obtained in 52% yield. Crystals were suitable for X-ray crystallography. ^{1}H NMR (δ, ppm, CD$_2$Cl$_2$): 2.64 (s, 3H, C$_6$H$_5$−*C*H$_3$), 7.79 (b, 5H, *C*$_6$H$_5$−CH$_3$) ^{13}C NMR (δ, ppm, CD$_2$Cl$_2$): 22.15(s, C$_6$H$_5$-*C*H$_3$), 139.76 (*ipso*, *C*$_6$H$_5$−CH$_3$), 129.87 (*o*, *C*$_6$H$_5$−CH$_3$), 130.70 (*m*, *C*$_6$H$_5$−CH$_3$), 126. 94 (*p*, *C*$_6$H$_5$−CH$_3$). ^{19}F NMR (δ, ppm, CD$_2$Cl$_2$): −73.74 (s, *C*F$_3$). UV−vis (toluene) (λ_{max}, nm (ϵ_M, M^{-1} cm^{-1})): 547 (300), 598 (430). UV−vis (THF) (λ_{max}, nm (ϵ_M, M^{-1} cm^{-1})): 479 (110), 482 (110), 522 (200), 544 (230), 599 (300). Anal. Calcd for $C_{46}H_{28}O_4F_{24}Tl_2Co$ (**8b**·2 toluene): C, 35.23; H, 1.80; F, 29.07. Found: C, 35.04; H, 1.71; F, 29.22. μ_{eff} (Evans' method) = 6.06μ_B.

(Me$_4$N)$_2$[Co(OAr^F)$_4$], 9. In the drybox, 1 equiv of [Tl$_2$Co(OAr^F)$_4$], **8a**, (100 mg, 0.8334 mmol) was slurried in CH$_2$Cl$_2$, and 2 equiv of Me$_4$NI (33.5 mg, 0.833 mmol) was added while the

Table 1. Summary of X-ray Crystallographic Data for Copper Complexes

	1b	3	4	5	6
formula	$C_{56}H_{60}CuF_{24}K_2O_{16}$	$C_{72}H_{40}CuF_{20}O_4P_2$	$C_{56}H_{72}CuF_{20}N_2O_4$	$C_{36}H_{32}CuF_{20}N_2O_4$	$C_{61}H_{80}Cl_2Cu_2K_2O_{18}$
formula weight	1586.78	1474.52	1280.70	1000.18	1377.43
space group	$P\bar{1}$	$P2_1/c$	$Pbca$	$P2_1/c$	$P2_1/n$
a, Å	12.3827(13)	12.0060(12)	15.0601(9)	12.5488(7)	15.205(5)
b, Å	13.0390(14)	18.7195(18)	17.5377(11)	12.4550(7)	21.230(8)
c, Å	13.2356(14)	14.9767(15)	22.8468(15)	14.0038(8)	20.040(7)
α, deg	100.929(2)				-
β, deg	112.815(2)	108.055(2)		114.282(1)	91.224(7)
γ, deg	111.913(2)				
V, Å^3	1682.1(3)	3200.2(5)	6034.3(7)	1995.10(19)	6468(4)
Z, Z'	1, 0.5	2, 0.5	4, 0.5	2, 0.5	4, 1
crystal color, habit	green, block	green, block	green, block	green, block	black, block
ρ(calc), g cm^{-3}	1.566	1.530	1.410	1.665	1.415
μ(Mo Kα), cm^{-1}	5.78	5.01	4.69	6.83	9.37
temp, K	293(2)	293	218(2)	218(2)	218(2)
reflections measured	10 718	15 445	36 069	14 444	38 465
reflections ind	7145 (R_{int} = 0.0200)	5015 (R_{int} = 0.0617)	7277 (R_{int} = 0.0313)	4751 (R_{int} = 0.0242)	11384 (R_{int} = 0.0368)
$R(F)$, %[a]	10.50	5.20	5.05	3.47	4.98
$R(wF^2)$,%[b]	28.85	9.63	15.09	9.58	12.95

[a] $R = \sum||F_o| - |F_c||/\sum|F_o|$. [b] $R(\omega F^2) = \{\sum[\omega(F_o^2 - F_c^2)^2]/\sum[\omega(F_o^2)^2]\}^{1/2}$; $\omega = 1/[\sigma^2(F_o^2) + (aP)^2 + bP]$, $P = [2F_c^2 + \max(F_o,0)]/3$.

solution was stirring. A dark blue solution with yellow precipitate was formed. After the solution was stirred overnight, a dark brown-purple precipitate had formed around the yellow precipitate. THF was added to dissolve the dark brown-purple precipitate. After the addition of THF, the solution turned purple and was filtered through Celite, and the solvent was removed in vacuo. A purple solid remained, which was triturated three times with 2 mL of hexane. The product was dissolved in a minimum amount of THF, filtered, layered with hexane for recrystallization, and stored at −30 °C. After 1 day, the product was collected via filtration, leaving a light purple solid in 82% yield. ^{1}H NMR (δ, ppm, {$(CD_3)_2CO$}): 2.481 (s, 12H, NCH_3). ^{13}C{^{1}H} NMR (δ, ppm, {$(CD_3)_2CO$}): 69.29 (s, CH_3). UV−vis (CH_2Cl_2) (λ_{max}, nm (ϵ_M, M^{-1} cm^{-1})): 539 (200), 592 (320). Anal. Calcd for $C_{32}H_{24}N_2O_4F_{20}Co$: C, 40.91; H, 2.57; N 2.98. Found: C, 40.89; H, 2.50; N 2.91. μ_{eff} (Evans' method) = 4.56μ_B.

$[Cp_2Co]_2[Co(OAr')_4]$, 10. A portion of Cp_2Co (300 mg, 1.586 mmol) was dissolved in 6 mL of CH_2Cl_2 to give a dark red-brown solution. A syringe was used to add 1.33 equiv of HOAr′ (322 μL, 2.115 mmol) with no obvious color changes. The solution was sealed in an ampule and heated to reflux with an oil bath. A dark green color was observable within 2 h, and the heating was allowed to continue overnight. Upon completion, the solvents were removed in vacuo, and the oily green product was washed with pentanes and dried in vacuo. The oil was recrystallized from toluene and hexanes. (**N. B.** Metathesis reactions using 2:1 ratios of $[Cp_2Co]PF_6$ and $[Co(OAr')_4]^{2-}$ salts in CH_3CN/THF showed colors consistent with **10**, but recrystallization attempts reformed the starting material mixture.) ^{1}H NMR (δ, ppm, {$(CD_3)_2CO$}): 6.59 (v. br). ^{13}C{^{1}H} NMR (δ, ppm, {$(CD_3)_2CO$}): 87.55 (HC Cp). ^{19}F NMR (δ, ppm, {$(CD_3)_2CO$}): −66.80 (CF_3). UV−vis (THF) (λ_{max}, nm (ϵ_M, M^{-1} cm^{-1})): 315 (17,160), 615 (510), 662 (470). Anal. Calcd for $C_{52}H_{32}O_4F_{24}Co_3$: C, 46.14; H, 2.38. Found: C, 46.16; H, 2.12. μ_{eff} (Evans' method) = 4.67μ_B.

{K(18-crown-6)}$_2$[$Co_2(\mu_2$-$OC_6H_5)_2(OC_6H_5)_4$], 11. A portion of CoI_2 (88.7 mg, 0.29 mmol) was dissolved in 6 mL of THF to give a blue-green solution. To this solution, 3 equiv of KOPh (120 mg, 0.91 mmol) was added, giving an intense blue color. The reaction mixture was stirred for 3 h at room temperature after which time there appeared some slight turbidity. The reaction mixture was filtered through Celite to remove (presumed) KI with the addition of 4 mL of additional THF. The filtrate was evaporated to dryness under reduced pressure and triturated twice with 5 mL hexanes each, to give the crude product as a blue powder. Subsequently, 2 equiv of 18-crown-6 (150 mg, 0.57 mmol) were added to the crude product in 15 mL of CH_2Cl_2 and stirred for 1 h. The subsequent blue solution was filtered through Celite, concentrated to dryness, and recrystallized from a slow diffusion of hexanes into CH_2Cl_2 affording blue crystals with a blocklike habit (60 mg, 55% yield). ^{1}H NMR (δ, ppm, {$(CD_3)_2CO$}): 3.787 (s, 24H, CH_2). ^{13}C{^{1}H} NMR (δ, ppm, {$(CD_3)_2CO$}): 70.95 (s, CH_2). UV−vis (THF) (λ_{max}, nm (ϵ_M, M^{-1} cm^{-1})): 496 (260), 598 (440), 659 (540). (Anal. Calcd For $C_{60}H_{78}O_{18}K_2Co_2$: C, 56.15; H, 6.13. Found: C, 56.22; H, 6.18. μ_{eff} (Evans' method) = 5.68μ_B.

$(Ph_4P)_2[CoCl_2(OAr^F)_2]$, 12. A portion of $CoCl_2$ (83.8 mg, 0.6453 mmol) was reacted with 4 equiv of $TlOAr^F$ (1.00 g, 2.581 mmol) in 25 mL of toluene and allowed to stir overnight. A cobalt blue color evolved slowly with the formation of some white precipitate. The reaction was filtered through Celite the following day to remove the precipitate, and the blue solution was concentrated to dryness. A 2-equiv portion of Ph_4PCl (484 mg, 1.291 mmol) and 20 mL of CH_2Cl_2 were added to the crude product. Formation of white solid was observed instantly, and the reaction was allowed to stir overnight. The presumed TlCl precipitate was again removed through Celite, and the bright blue oily product was recrystallized from CH_2Cl_2 and hexanes. Crystalline material required slow growth over several days from room temperature solutions, and 173 mg (22.3% yield) was eventually obtained. ^{1}H NMR (δ, ppm, {$(CD_3)_2CO$}): 7.559 (br, CH), 7.590 (br, CH), 7.632 (br, CH), 7.802 (br, CH). ^{13}C{^{1}H}NMR (δ, ppm, {$(CD_3)_2CO$}): 118.61 (*i*, d, J_{CP} = 89.9 Hz), 131.52 (*o*, d, J_{CP} = 12.8 Hz), 136.08 (*m*, d, J_{CP} = 10.1 Hz), 136.51 (*p*, s). UV−vis (CH_2Cl_2) (λ_{max}, nm (ϵ_M, cm^{-1} M^{-1})): 350 (310), 635 (270), 674 (270). Anal. Calcd for $C_{60}H_{40}O_2F_{10}P_2Cl_2Co$: C, 61.35; H, 3.43. Found: C, 61.22; H, 3.37. μ_{eff} (Evans' method) = 4.45μ_B.

X-ray Crystallography. A summary of crystal data collection and refinement parameters for all compounds are given in Tables 1 and 2. X-ray diffraction data were collected on either a Bruker SMART[51] APEX CCD (**7b**, **12**) or a Siemens P4 diffractometer equipped with a SMART[51] Apex CCD detector (**1b**, **3**, **4**, **5**, **6**, **7a**, **10**, **11**). Space groups and lattice symmetries were determined through inspection of systematic absences and intensity statistics in **1b**. All data sets were corrected for absorption using the program

(51) *SMART: Software for the CCD Detector System*; Bruker AXS: Madison, WI, 2000.

Table 2. Summary of X-ray Crystallographic Data for Cobalt Complexes

	7a	7b	10	11	12
formula	$C_{56}H_{66}CoF_{20}K_2O_{18}$	$C_{56}H_{60}CoF_{24}K_2O_{16}$	$C_{52}H_{32}Co_3F_{24}O_4$	$C_{31}H_{41}Cl_2CoKO_9$	$C_{60}H_{40}Cl_2CoF_{10}O_2P_2$
formula weight	1540.19	1582.17	1353.57	726.57	1174.69
space group	*C*2/*c*	*C*2/*c*	*C*2/*c*	$P2_1/n$	$P2_1/c$
a, Å	22.0161(10)	23.3983(13)	24.202(3)	13.487(4)	19.7866(13)
b, Å	16.0513(7)	12.7964(6)	13.9911(17)	15.672(4)	14.2273(10)
c, Å	19.1081(9)	24.0070(13)	17.1697(19)	16.844(4)	18.6950(13)
α, deg					
β, deg	101.730(1)	109.109(2)	114.678(2)	105.970(6)	95.751(1)
γ, deg					
V, Å^3	6611.5(5)	6792.0(6)	5282.9(11)	3422.9(15)	5236.3(6)
Z, *Z*′	4, 0.5	4, 0.5	4	4, 0.5	4, 1
crystal color, habit	blue, block	blue, block	green, block	green, block	blue, block
ρ(calc), g cm^{-3}	1.547	1.547	1.702	1.410	1.490
μ(Mo Kα), cm^{-1}	5.09	5.03	10.61	8.29	5.71
temp, K	218(2)	150(2)	293(2)	218(2)	100(2)
reflections measured	21 480	21 302	17 151	18 579	33 218
reflection ind	6485 (R_{int} = 0.0358)	7978 (R_{int} = 0.0288)	5957 (R_{int} = 0.0435)	5378 (R_{int} = 0.0888)	12328 (R_{int} = 0.0379)
$R(F)$, %[a]	6.17	8.36	9.67	6.80	5.27
$R(wF^2)$,%[b]	15.55	21.21	29.37	15.09	13.86

[a] $R = \sum||F_o| - |F_c||/\sum|F_o|$. [b] $R(\omega F^2) = \{\sum[\omega(F_o^2 - F_c^2)^2]/\sum[\omega(F_o^2)^2]\}^{1/2}$; $\omega = 1/[\sigma^2(F_o^2) + (aP)^2 + bP]$, $P = [2F_c^2 + \max(F_o,0)]/3$.

SADABS.[52] The structures were solved using direct methods or the Patterson function and difference map techniques and were refined by full-matrix least-squares procedures on F^2. All non-hydrogen atoms were refined with anisotropic displacement parameters. The H atoms were treated as idealized contributions except **5** where they were located in the Fourier difference map and refined with isotropic thermal parameters. One CF_3 group in **10**, all the CF_3 groups in **7b**, one terminal CH_3 group in **4**, and the O(6) atom in **7a** are disordered over two positions. Highly disordered CH_2Cl_2 solvent molecules in **6** were verified by the SQUEEZE program.[53] Corrections of the X-ray data with 155 electrons/cell were close to the required value of 168 electrons/cell. All software and sources of scattering factors are contained in the SHELXTL program package.[54]

Electrochemistry. Cyclic voltammetry experiments were carried out in CH_2Cl_2 with 1.0 M ($^nBu_4N$)PF_6 (recrystallized three times from CH_2Cl_2) with analyte concentrations of approximately 2.0 mM. Experiments were performed in a nitrogen-filled drybox, using a three-electrode cell with all leads connected through binding posts to an external EG&G model 273a potentiostat (Princeton Applied Research) run by a personal computer with M270/250 Research Electrochemistry software, version 4.30. A platinum (2 mm diameter) working electrode, Ag wire quasi-reference electrode, and Pt counter electrode were used. The working electrode was cleaned between experiments using 1 mm Al_2O_3 slurry (Buehler), carefully dried, and returned to the drybox. Scan rates were in the range 20−500 mV/s. Solutions of [K{18-crown-6}(OAr^F)] and [K{18-crown-6}(OAr′)] were prepared by adding equimolar amounts of the appropriate KOAr salt and 18-crown-6.

Results and Discussion

In our research group, we were interested in preparing homoleptic aryloxide anions that were neither coordinatively nor sterically saturated at the metal center. We chose two highly fluorinated aryloxides for this purpose, pentafluorophenoxide, $OC_6F_5^-$ (OAr^F), and bis-3,5-trifluoromethylphenoxide, $OC_6H_3(CF_3)_2^-$ (OAr′). We anticipated that fluorination of the aryl rings, which should result in decreased electron density at oxygen, would reduce the tendency toward bridging and formation of oligomeric or polymeric materials. Other electronic effects may also play a role. (E.g., for OAr^F, there is substantial participation of the peripheral F atoms in the π system of the ring, whereas for OAr′ no such effects are formally present.) The inductive influence of fluorination of some or all of the carbon atoms in the two phenols is reflected in the pH values for both materials, which are 8.42 for $HOAr^F$ [55] and 8.26 for HOAr′,[55] compared to 9.78 for phenol[55] and 10.20 for 3,5-dimethylphenol.[56] Fluorination also reduces the likelihood of unwanted C−H activation and alters the possibility of ligand reduction or oxidation reactions (such as preventing oxidation to the quinone) in comparison to the perprotio-congeners.

Syntheses. The tetrakisphenolate anion $[M(OAr)_4]^{2-}$ is formed readily by simple metathesis reactions as shown in Figures 1 and 2. The potassium phenoxides are reacted in THF with $^1/_4$ equiv of $CuBr_2$. Addition of 2 equiv of 18-crown-6 in CH_2Cl_2 and separation of residual KBr give the compounds {K(18-crown-6)}$_2$[Cu(OAr^F)$_4$], **1a**, and {K(18-crown-6)}$_2$[Cu(OAr′)$_4$], **1b**, in good yield. Syntheses of the [Tl_2Cu(OAr)$_4$] complexes proceed under different conditions. Unlike the potassium phenoxides, the thallium compounds $TlOAr^F$ and TlOAr′ are quite soluble in toluene. The synthetic result is that $CuBr_2$ reacts readily in toluene with 4 equiv of TlOAr to form [Tl_2Cu(OAr^F)$_4$], **2a,** and [Tl_2Cu(OAr′)$_4$], **2b**. Analytically pure **2a** was recrystallized from toluene and hexane to give a fine brown powder, and **2b** was recrystallized with THF solvation. The thallium cations can be metathesized easily from **2a** and **2b** to form a variety of other A_2[Cu(OAr)$_4$] compounds, including the Ph_4P^+ derivative (Ph_4P)$_2$[Cu(OAr^F)$_4$], **3**, via exchange with Ph_4PI, demonstrating the robust nature of the phenolate anion

(52) Sheldrick, G. M. *SADABS: Area Detector Absorption Correction*; University of Göttingen: Göttingen, Germany, 2001.
(53) Van der Sluis, P.; Spek, A. L. *Acta Crystallogr.* **1990**, *A46*, 194−201.
(54) Sheldrick, G. M. *SHELXTL: Program Library for Structure Solution and Molecular Graphics*; Bruker AXS: Madison, WI, 2000.
(55) Abraham, M. H.; Duce, P. P.; Morris, J. J.; Taylor, P. J. *J. Chem. Soc., Faraday Trans. 1* **1987**, *83*, 2867−81.
(56) *The Chemistry of the Hydroxyl Group*; Patai, S., Ed.; Interscience: London, New York, 1971; Part 1.

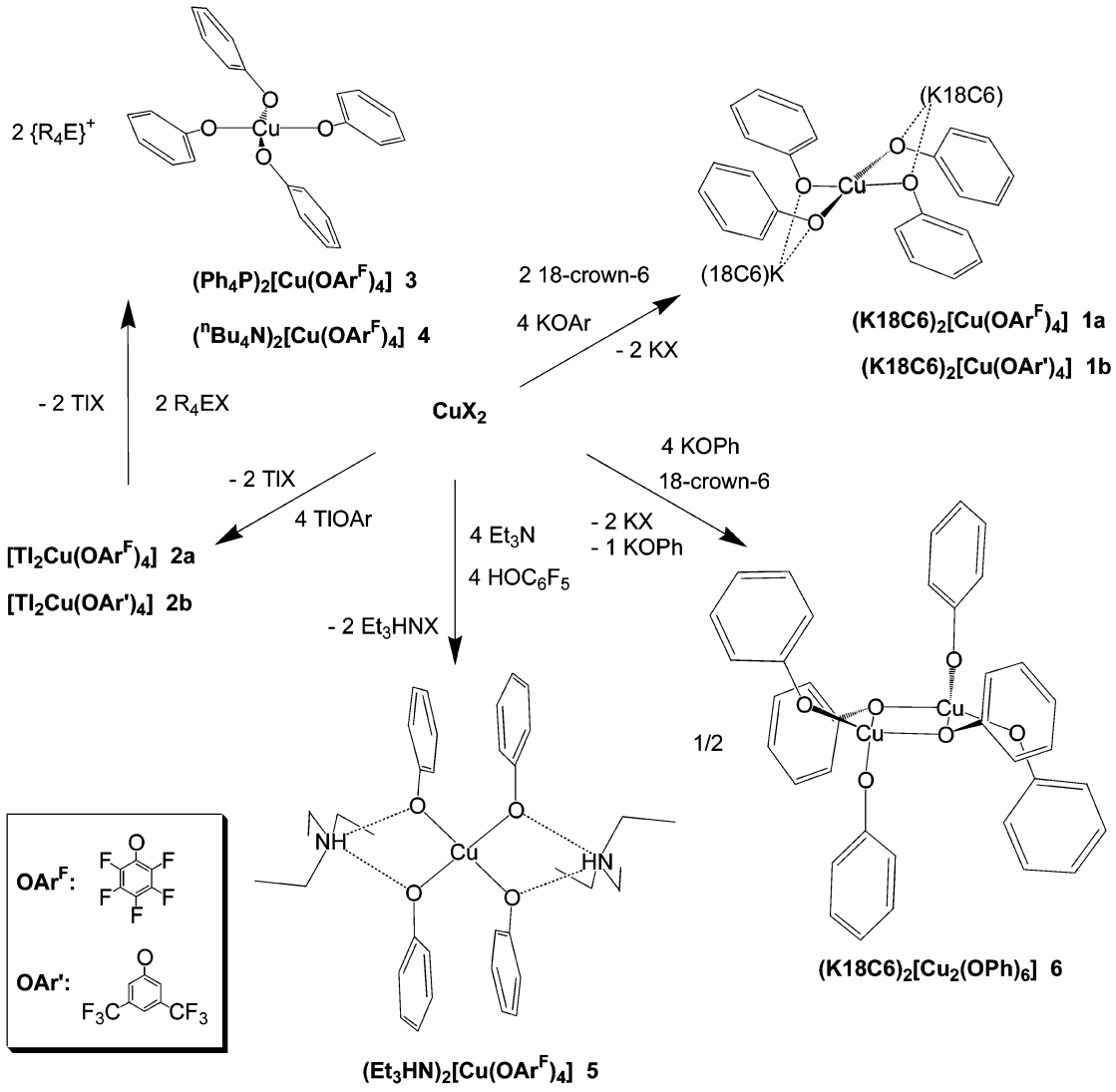

Figure 1. Syntheses of homoleptic copper phenolate anions $[Cu(OAr)_4]^{2-}$ and related compounds.

under these conditions. The related compound $(^nBu_4N)_2[Cu(OAr^F)_4]$, **4**, was prepared from $(^nBu_4N)_2[CuCl_4]$[35] and $TlOAr^F$.

The analogous reactions were studied with KOPh and TlOPh. Reaction of 4 equiv of TlOPh with 1 equiv of $CuBr_2$ in THF yielded only insoluble material, suggesting oligomers or polymers, whereas **2a** and **2b** are significantly soluble not only in THF but also in toluene. Reaction of KOPh and addition of 18-crown-6 with a ligand−metal ratio of 4:1 yielded the dinuclear complex $\{K(18\text{-crown-}6)\}_2[Cu_2(\mu\text{-}OPh)_2(OPh)_4]$, **6**, and residual KOPh. Compound **6** (as well as **11**) was subsequently synthesized from a 1:3 ratio of Cu(II) (Co(II) for **11**) and $KOAr^F$ (Experimental Section). These control experiments demonstrate that substantial fluorination on the phenyl ring allows the formation of mononuclear compounds under conditions in which nonfluorinated phenoxide ligands yield dimeric or insoluble species.

The $[Cu(OAr^F)_4]^{2-}$ anion can be formed also by the deprotonation of the fluorinated phenols with amines to form the ammonium salt $(Et_3HN)_2[Cu(OAr^F)_4]$, **5**. The reaction shown in Figure 1 gave good yields of **5** under *aerobic* conditions, with no care to exclude water or oxygen. Control experiments with HOPh led to intractable, insoluble oily brown materials. These intractable mixtures could be the results of phenol polymerization[57] and are under further investigation.

The cobalt derivatives can be synthesized in a similar manner. Reaction of CoI_2 with an appropriate stoichiometric quantity of $KOAr^F$ and 18-crown-6, as for **1a** and **1b**, resulted in facile formation of $\{K(18\text{-crown-}6)\}_2[Co(OAr^F)_4]$, **7a**, and $\{K(18\text{-crown-}6)\}_2[Co(OAr')_4]$, **7b**, in good yield. The related thallium $[Tl_2Cu(OAr)_4]$ complexes, **8a** and **8b**, were prepared in toluene, analogous to **2a** and **2b**, as shown in Figure 2. Reaction of $CoCl_2$ under similar conditions yields some TlCl precipitate and a cobalt-blue product but also unreacted $TlOAr^F$. Treatment of the cobalt product of these conditions with Ph_4PCl and removal of TlCl led to isolation of $(Ph_4P)_2[CoCl_2(OAr^F)_2]$, **12**, presumably through an intermediate with the stiochiometry $\{Tl_2CoCl_2(OAr^F)_2\}$. Complete substitution at cobalt required CoI_2 as a starting

(57) Aromi, G.; Gamez, P.; Kooijman, H.; Spek, A. L.; Driessen, W. L.; Reedijk, J. *Eur. J. Inorg. Chem.* **2003**, 1394−1400.

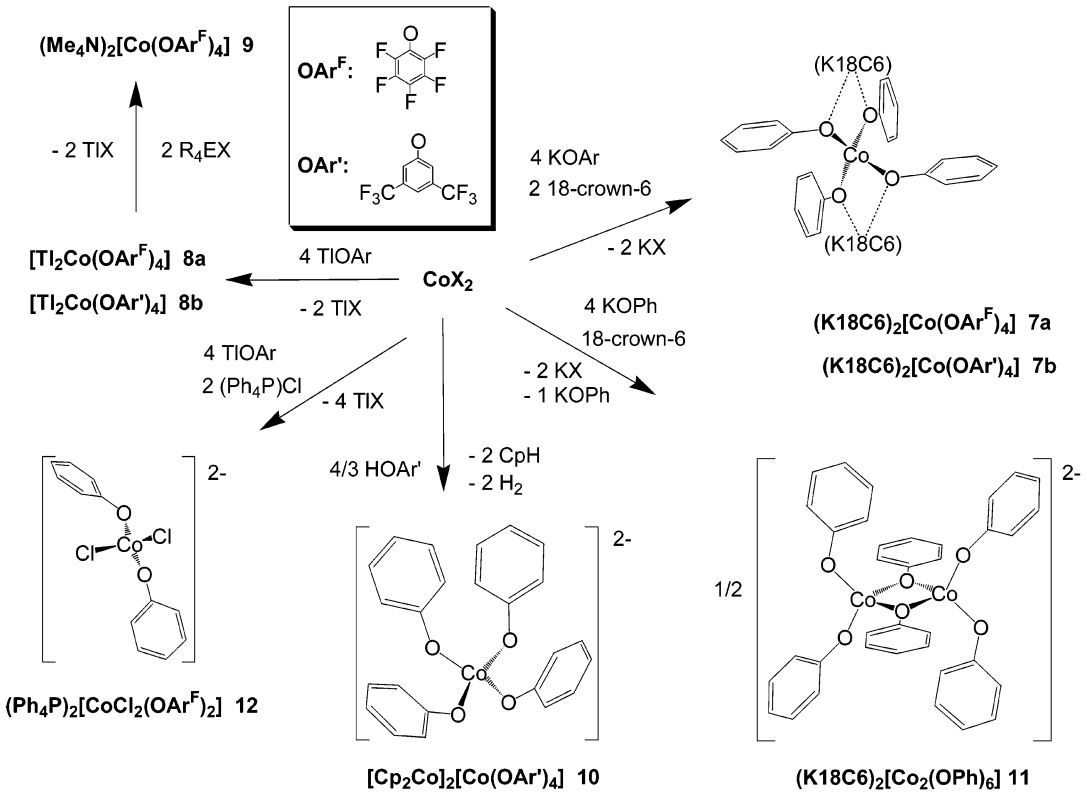

Figure 2. Syntheses of homoleptic cobalt phenolate anions $[Co(OAr)_4]^{2-}$ and related compounds.

material which is quite soluble in THF, unlike $CoCl_2$. In the reaction between $TlOAr^F$ and $CoCl_2$, either the driving force of TlCl lattice formation is not enough to completely breakup the $CoCl_2$ lattice or the reaction kinetics are too slow to be synthetically useful. In contrast, Co−I bond cleavage and TlI precipitation are complete within hours of the reaction between $TlOAr^F$ and CoI_2. Metathesis of **8a** with Me_4NI resulted in elimination of yellow TlI and formation of $(Me_4N)_2[Co(OAr^F)_4]$, **9**, analogous to the synthesis of **3**, vide supra.

With regard to metal chlorides as starting materials, $CuCl_2$ works just as well as $CuBr_2$ in the preparation of $[Cu(OAr)_4]^{2-}$ species. Reaction of $CoCl_2$ with either KOAr or TlOAr, however, led to residual aryloxide and incomplete substitution as demonstrated with the preparation of **12**. Because use of CoI_2 solved this problem, we suspect that bridging in CoX_2 is less strong with the heavier halides but have not made a detailed study of this phenomenon.

The cobalticenium compound $[Cp_2Co]_2[Co(OAr')_4]$, **10**, was discovered as a byproduct in the original preparation of $[Cp_2Co][Ar'O\cdots H\cdots OAr']$[34] and was synthesized again by the direct route reported in the Experimental Section. Cobaltocene (3 equiv) is reacted with 4 equiv of HOAr′, resulting in good yields of **10**. The reaction stoichiometry suggests concomitant formation of 2 equiv of cyclopentadiene from the protonation of two Cp ligands on the same cobalt center, which subsequently acquires four phenolate

$$3[Cp_2Co] + 4HOAr' \rightarrow [Cp_2Co]_2[Co(OAr')_4] + 2CpH + 2H_2$$

ligands. The other two $[Cp_2Co]$ equivalents are oxidized to $[Cp_2Co]^+$ and 2 mol of H_2 is produced. A ^1H NMR study of the reaction (Figure S1) is consistent with this stoichiometry, although no H_2 was detected. Oxidation of $[Cp_2Co]$ to $[Cp_2Co]^+$ with Brønsted acids is well precedented.[58,59] The compound is initially separated as a blue-green oil and is crystallized only over a period of weeks.

These $A_2[M(OAr)_4]$ complexes are the first homoleptic phenolate anions of late transition metal ions to be structurally and spectroscopically characterized. A previous report of some $[M(OAr^F)_4]^{2-}$ anions provided spectroscopic characterization[60] and proposed metal coordination[61] geometries, some of which are shown to be incorrect (vide infra). An earlier report[62] exists of the compounds $Li_2Co(OPh)_4\cdot 4THF$, $Na_2Co(OPh)_4\cdot 5THF$, and $K_2Co(OPh)_4\cdot 0.75THF$ but no structural characterization was performed, and substantial color changes from blue to red were observed upon loss of THF, suggesting metal coordination environment changes from tetrahedral to octahedral, vide infra. No data were provided to distinguish $M_2[Co(OPh)_4]$ structures from [MOPh]/$[MCo(OPh)_3]$ mixtures. The $Li_2Co(OPh)_4$ structures that are blue in the solid state become red (assumed to be octahedral) when dissolved in THF.[63] This behavior is in distinct contrast to compound **11** reported herein. Magnetic data also sug-

(58) Wilkinson, G.; Pauson, P. L.; Cotton, F. A. *J. Am. Chem. Soc.* **1954**, *76*, 1970−1974.
(59) Wilkinson, G.; Cotton, F. A.; Birmingham, J. M. *J. Inorg. Nucl. Chem.* **1956**, *2*, 95−113.
(60) Hollebone, B. R.; Nyholm, R. S. *J. Chem. Soc. A* **1971**, 332−337.
(61) Hollebone, B. R. *J. Chem. Soc. A* **1971**, 481−486.
(62) Ibrahim, A. I.; Gaube, W.; Kalies, W.; Witt, B. *J. Prakt. Chem.* **1991**, *333*, 397−406.
(63) El-Behairy, M.; Ibrahim, A. I.; Emara, A. A. A.; Tawfic, T. A. *J. Chem. Res., Synop.* **1996**, 22.

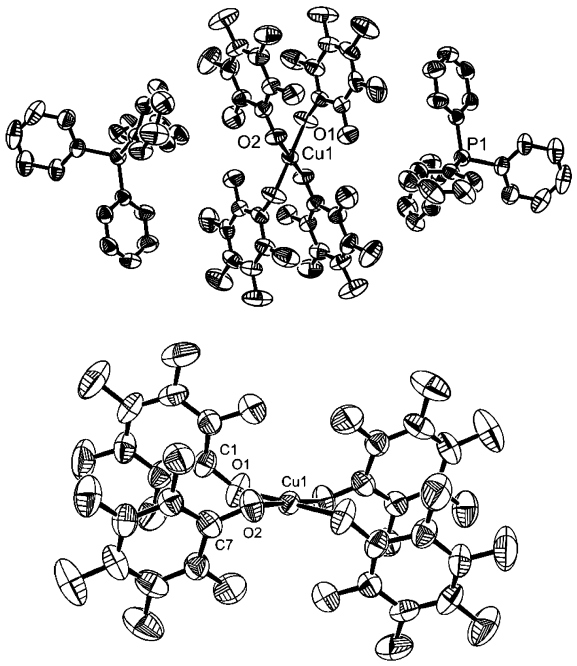

Figure 3. ORTEP diagrams of $(Ph_4P)_2[Cu(OAr^F)_4]$, **3**, (top) and anion alone (bottom). The copper atom sits on an inversion center. Hydrogen atoms have been omitted for clarity. Selected distances and angles: Cu(1)−O(1) = 1.912(3) Å, Cu(1)−O(2) = 1.926(3) Å, Cu−O−C_{avg} = 124.0(8)°. Ellipsoids are shown at the 50% probability level.

gested that these compounds did not contain $[M(OPh)_4]^{2-}$ cobalt centers.

A study of several $[Al(OR_F)_4]^-$ "superweak" anions of Lewis acid catalysts[64] demonstrated a linear relationship between the pK_a of the fluoro alcohol and the Lewis basicity of the aluminate anion. Analogously, the lower pK_a values of $HOAr^F$ and HOAr′ versus HOPh and $HOC_6H_3(CH_3)_2$ seem to reduce the basicity of the $[M(OAr)_4]^{2-}$ anions and thus prevent the bridging behavior and favor mononuclear anions whose structures are described in detail below.

Structural Characterization. First we discuss the structural features of the $[M(OAr)_4]^{2-}$ anions with the completely uncoordinating cations and then describe structures with cations showing some associative interaction. Crystallographic data collection parameters for the copper compounds are summarized in Table 1 and those for the cobalt compounds, in Table 2. Selected distances and angles are collected in Tables 3 (Cu) and 4 (Co).

Two different salts of the uncoordinated $[Cu(OAr^F)_4]^{2-}$ anion, $(Ph_4P)_2[Cu(OAr^F)_4]$, **3,** and $(^nBu_4N)_2[Cu(OAr^F)_4]$, **4,** have been crystallographically characterized. The cation and anion of **3** are shown in Figure 3, and those of **4** are shown in Figure S2. Both copper centers in **3** and **4** exhibit the same approximately square planar geometry. Each copper center is coplanar with the four oxygen atoms that lie at the corners of a rectangle having sides of 2.644(5) and 2.780(5) Å in the case of **3** and of 2.653(3) and 2.797(3) Å in **4**. The longer side of the rectangle, the O1···O2 vector in Figure 3, is the side on which the perfluorophenyl groups arrange themselves. The O−Cu−O angles are also slightly different from 90°, with the longer sides of the rectangle subtending wider angles. In **3**, the phenyl rings are staggered with the shortest distance of 2.988(6) Å between the two ortho atoms, C1 and C7. There are no close contacts in **3** or **4** with either of the structurally unexceptional Ph_4P^+ or $^nBu_4N^+$ cations. The average Cu−O distances in **3** and **4** are 1.919(8) and 1.928(4) Å, respectively, and the average O−C distances and Cu−O−C angles are 1.302(5) and 1.299(4) Å and 124.0(9) and 125.7(2)° in **3** and **4**, respectively. A search of the Cambridge Structural Database (CSD)[65] for Cu−phenoxide structures in which the phenoxide ligand is neither bridging nor part of a chelate ring yielded 29 structures and 34 crystallographically independent Cu−O−Ar linkages. Among these compounds the average parameters are 1.93(15) Å for the Cu−O distances, 1.32(2) Å for the O−C distances, and 128(7)° for the Cu−O−C angles. Thus, the average Cu−O and O−C bond lengths in compounds **3** and **4** (see Table 3) are comparable with the average values for these bond lengths.

Single-crystal X-ray diffraction studies revealed similar geometries for the anions of $[K\{18\text{-crown-}6\}]_2[Cu(OAr^F)_4]$, **1a**, and $[K\{18\text{-crown-}6\}]_2[Cu(OAr')_4]$, **1b**. The structure of only **1b**, Figure 4, is reported here in detail because disorder in the cation of several crystals of **1a** resulted in a structure of unpublishable quality, though the connectivity of the structural units present in the crystal were consistent with the chemical formulation.[66] In **1b**, the copper atom has an approximately square-planar geometry in the center of four oxygen donors that form a rectangle with sides 2.662(5) and 2.797(5) Å, similar to the analogous distances in **3** and **4**. The greater steric bulk of the OAr′ anion does not permit the adjacent phenoxides to come into such close contact as with OAr^F, however. The C(11)···C(21) distance in **1b** is 4.279(7) Å. The shorter sides of the rectangle are each loosely bridged by a $\{K(18\text{-crown-}6)\}^+$ cation between aryloxide oxygen atoms. These interactions are weak as demonstrated by the long K−O(aryloxide) average distance of 2.76(5) Å, by an absence of shortening in the O···O distance in the anion and no significant lengthening of the Cu−O bonds in contrast to that observed in **6** (vide infra). The average K···O (noncrown) distance from 68 examples in the CSD of $\{K(18\text{-crown-}6)\}^+$ cations with two additional oxygen atom donors is 2.8(2) Å. In **1b**, the unique Cu−O distances are 1.917(3) and 1.944(4) Å, and the Cu−O−C angles have a range of 127.7(3) to 130.2(3)°. These parameters are not significantly different from the purely monodentate aryloxides in **3** and **4** described above, demonstrating that the potassium atoms exert little perturbation on the anion geometry. The data for **1a** show a structure quite similar to **1b**, an approximately square-planar Cu(II) center and long K−O (aryloxide) contacts on two sides of the rectangle. The $\{K(18\text{-crown-}6)\}^+$ cations in **1a** bridge the short edges of the rectangle away from the OAr^F rings, analogous to the ammonium cations in **5**, vide infra. Previous

(64) Ivanova, S. M.; Nolan, B. G.; Kobayashi, Y.; Miller, S. M.; Anderson, O. P.; Strauss, S. H. *Chem.—Eur. J.* **2001**, *7*, 503−510.

(65) Allen, F. H. *Acta Crystallogr.* **2002**, *B58*, 380−388.

(66) *Pnnm*, *a* = 9.2001 Å, *b* = 17.6783 Å, *c*= 19.2815 Å.

Table 3. Selected Interatomic Distances, Bond Lengths, and Angles for Copper Compounds[a]

compound	distances	(Å)	angles	(deg)
1b	Cu1−O1	1.917(3)	O1−Cu1−O2	92.83(15)
	Cu1−O2	1.944(4)	O1−Cu1−O2_2	87.17(15)
	O1···O2	2.797(5)	Cu1−O1−C11	127.7(3)
	O1···O2_2	2.662(5)	Cu1−O2−C21	130.2(3)
	O1−C11	1.315(6)		
	O2−C21	1.306(6)		
	C11···C21	4.279(7)		
	K1−O1	2.793(4)		
	K1−O2	2.718(4)		
3	Cu1−O1	1.912(3)	O1−Cu1−O2	92.83(12)
	Cu1−O2	1.926(3)	O1−Cu1−O2_2	87.17(12)
	O1···O2	2.780(5)	Cu1−O1−C1	123.2(3)
	O1···O2_2	2.644(5)	Cu1−O2−C7	124.8(2)
	O1−C1	1.305(5)		
	O2−C7	1.298(5)		
	C1···C7	2.988(6)		
4	Cu1−O1	1.9243(16)	O1−Cu1−O2	86.98(7)
	Cu1−O2	1.9311(15)	O1−Cu1−O2_5	93.02(7)
	O1···O2	2.797(3)	Cu1−O1−C1	125.73(14)
	O1···O2_5	2.653(3)	Cu1−O2−C7	125.65(13)
	O1−C1	1.298(3)		
	O2−C7	1.300(3)		
	C1···C7	2.985(4)		
5	Cu1−O1	1.9195(10)	O1−Cu1−O2	95.27(5)
	Cu1−O2	1.9290(11)	O1−Cu1−O2_3	84.73(5)
	O1···O2	2.593(2)	Cu1−O1−C1	125.13(9)
	O1···O2_3	2.844(2)	Cu1−O2−C7	122.83(9)
	O1−C1	1.314(2)		
	O2−C7	1.313(2)		
	C1···C7_3	2.951(2)		
	O1···N1	2.950(2)		
	O2···N1	2.882(2)		
6	Cu1−O1	1.9473(19)	O1−Cu1−O2	77.73(8)
	Cu1−O2	1.9527(19)	O2−Cu1−O3	100.62(8)
	Cu1−O3	1.9046(19)	O3−Cu1−O4	89.35(8)
	Cu1−O4	1.8823(19)	O4−Cu1−O1	99.22(9)
	Cu2−O1	1.9577(19)	O2−Cu1−O4	158.62(9)
	Cu2−O2	1.9608(19)	O1−Cu1−O3	159.83(9)
	Cu2−O5	1.8835(19)	O1−Cu2−O2	77.30(8)
	Cu2−O6	1.8990(19)	O2−Cu2−O5	99.87(9)
	Cu1···Cu2	3.0483(9)	O5−Cu2−O6	89.55(9)
	O1···O4	2.917(3)	O6−Cu2−O1	99.64(9)
	O2···O3	2.968(2)	O1−Cu2−O5	159.85(9)
	O1···O6	2.947(3)	O2−Cu2−O6	160.04(9)
	O2···O5	2.943(2)	Cu1−O1−Cu2	102.64(9)
	O1···O2	2.447(2)	Cu1−O2−Cu2	102.32(9)
	O3···O4	2.663(3)	Cu1−O1−C1	122.22(17)
	O5···O6	2.664(3)	Cu1−O2−C7	122.93(15)
	O1−C1	1.358(4)	Cu1−O3−C13	120.52(17)
	O2−C7	1.355(3)	Cu1−O4−C19	124.93(18)
	O3−C13	1.326(3)	Cu2−O1−C1	122.36(16)
	O4−C19	1.322(4)	Cu2−O2−C7	122.57(16)
	O5−C25	1.318(4)	Cu2−O5−C25	122.40(18)
	O6−C31	1.324(4)	Cu2−O6−C31	120.47(17)
	K1−O3	2.743(2)		
	K1−O4	2.715(2)		
	K2−O5	2.792(2)		
	K2−O6	2.722(2)		

[a] Numbers in parentheses are estimated deviations of the last significant figure.

spectroscopic characterization of $(Et_4N)_2[Cu(OAr^F)_4]$ was used to propose a tetrahedral geometry.[61]

The structures of the four thallium salts, **2a**,[67] **2b**,[68] **8a**,[69] and **8b**,[70] have all been determined, have significantly more complicated bimetallic structures with bridging phenoxide ligands, and will be discussed in a separate publication.

Contacts between the cation and anion are also observed in $(Et_3HN)_2[Cu(OAr^F)_4]$, **5**. The structure in **5**, shown in Figure 5, is generally similar to the three discussed previ-

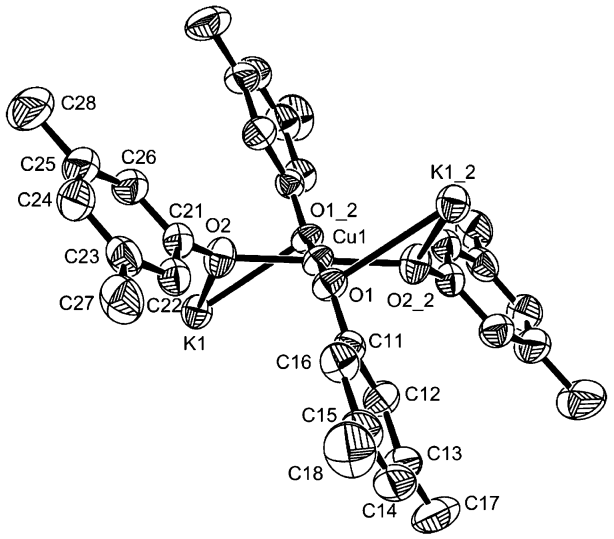

Figure 4. ORTEP diagram of the $[Cu(OAr')_4]^{2-}$ anion and K^+ cations from **1b**. The copper atom sits on an inversion center. Crown ether, hydrogen, and fluorine atoms have been omitted for clarity. Selected distances and angles: Cu(1)−O(1) = 1.917(3) Å, Cu(1)−O(2) = 1.944(4) Å, Cu−O−C_{avg} = 129(1)°. Ellipsoids are shown at the 50% probability level.

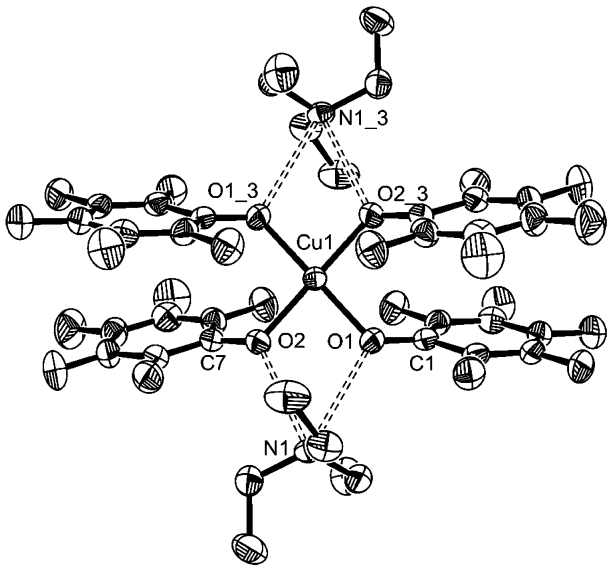

Figure 5. ORTEP diagram of $(Et_3NH)_2[Cu(OAr^F)_4]$, **5**, showing hydrogen bonding between cation and anion. The copper atom sits on an inversion center. Hydrogen atoms are omitted for clarity. Selected distances: Cu(1)−O(1) = 1.9195(10) Å, Cu(1)−O(2) = 1.9290(11) Å, O(1)···O(2) = 2.593(2) Å, O(1)···N(1) = 2.950(2) Å, O(2)···N(1) 2.882(2) Å. Ellipsoids are shown at the 50% probability level.

ously, except for the bifurcating hydrogen bonds between the Et_3HN^+ cations and the aryloxide oxygen atoms (Table 3) in which the average O−N distance is 2.916(4) Å, quite normal for such bonds.[71] The bridging proton was not located

(67) $P\bar{1}$, a = 14.858 Å, b = 20.1452 Å, c = 28.5113 Å, α = 96.734°, β = 94.611°, γ = 93.648°.
(68) $Pbcn$, a = 15.3095 Å, b = 30.0215 Å, c = 16.7395 Å.
(69) $P\bar{1}$, a = 11.7969 Å, b = 13.9222 Å, c = 25.2309 Å, α = 96.740°, β = 102.643°, γ = 96.954°.
(70) $P\bar{1}$, a = 11.8345 Å, b = 13.0593 Å, c = 15.9152 Å, α = 100.657°, β = 96.325°, γ = 113.222°.
(71) Jeffrey, G. A. *An Introduction to Hydrogen Bonding*; Oxford University Press: New York, 1997.

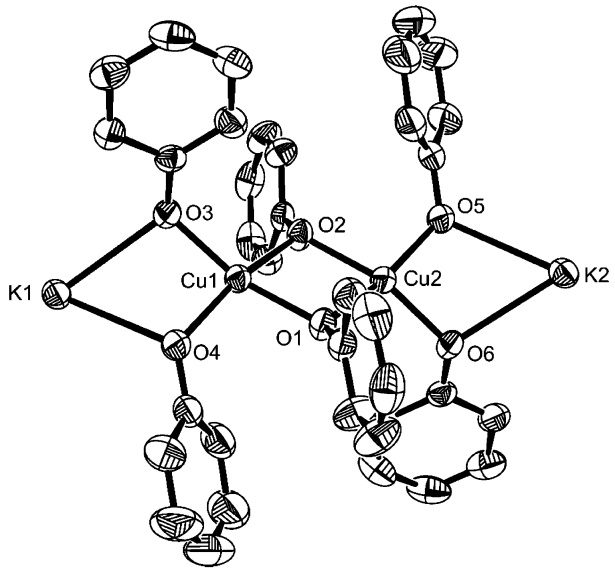

Figure 6. ORTEP diagram of the anion of $\{K(18\text{-crown-}6)\}_2[Cu_2(\mu\text{-OPh})_2(OPh)_4]$, **6**. Crown ether and hydrogen atoms are omitted for clarity. Selected distances and angles: Cu(1)−O(1) = 1.9473(19) Å, Cu(1)−O(3) = 1.9046(19) Å, Cu(1)···Cu(2) = 3.0483(9) Å, Cu(1)−O(1)−Cu(2) = 77.73(8)°. Ellipsoids are shown at the 50% probability level.

in the difference map but calculated. Again, the Cu atom is in the center of a rectangle with Cu−O distances close to 1.92 Å and edges differing slightly in length. The Et_3HN^+ ions bridge the short sides of the rectangle which are shorter by ∼0.25 Å, and the angles at Cu in the $Cu-O_4$ plane are close to 85° and 95°. In **1b**, **3**, and **4** the average difference in side length was ∼0.15 Å and the angles 3° removed from 90°, suggesting a small distortion of the anion by the hydrogen bonding cations. The Cu−O bond lengths in **5** are not longer than the other three phenolate anions however; thus the Et_3HN^+ cations, such as the $\{K(18\text{-crown-}6)\}^+$ cations, are not strongly bound to the aryloxide groups.

The small variations among Cu−O−C angles are detailed in Table 3 and show no correspondence with Cu−O bond lengths. Although the angles are significantly wider than a canonical tetrahedral angle, several other groups have established that no correlation exists between larger M−O−C(Ar) angles and shorter M−O distances that might suggest increased M−O bond order.[72] The CSD search detailed above demonstrates that angles more obtuse than 109.5° are quite common in such linkages.

In the dinuclear compound **6**, shown in Figure 6, each Cu(II) center is significantly distorted from square-planar geometry; the dihedral angle between the O(1)−Cu(1)−O(2) and O(3)−Cu(1)−O(4) planes is 30.19°, and the dihedral angle between the O(1)−Cu(2)−O(2) and O(5)−Cu(2)−O(6) planes is 28.94°. There are 20 compounds in the CSD with coordination pattern of $\{O_2Cu(\mu_2\text{-OR})_2CuO_2\}$, the majority of which have two square-planar Cu(II) centers. Only one compound has copper centers more distorted toward tetrahedral than **6**, namely, the linear compound $[Cu_4(\mu_2\text{-O}^t\text{Bu})_6\{O(CF_3)_3\}_2]$ in which the central two copper atoms have D_{2d} CuO_4 coordination and the two terminal Cu atoms have approximately C_{2v} CuO_3 coordination. Steric repulsions between bridging O^{t}Bu groups are likely responsible for the substantial distortion from square-planar geometry of the internal copper centers.[73] The ends of **6**, like **1a** and **1b**, are loosely coordinated to the two $\{K(18\text{-crown-}6)\}^+$ cations with an average distance from K−O of 2.74(3) (Å) (Table 3).

The terminal Cu−O(Ar) distances reported for **6** in Table 3 are well within the range of reported bond lengths for acyclic linkages in the literature (34 crystallographically independent described above) that have an average of 1.93(15) Å. The average Cu−O(terminal) distance is 1.892(11) Å, slightly shorter than the related distances in **1b**, **3**, **4**, and **5**, having the fluorinated aryloxides described above. These data suggest a correlation between the basicity of the ligand (measured by the pK_a of the parent alcohol) and the length of the M−O bond. The average μ_2-OAr distances (Å) in **6**, 1.955(6), are longer than those from the nonbridging phenoxides, as expected, and again consistent with literature range of 1.99(9). The average of Cu−O−C angles (deg) in the literature is 128(7) compared to 122.3(1.4) in **6** from Table 3. The Cu−O and O−C distances in **6** are also unexceptional and within the literature range. Again, there is no correlation between Cu−O−C angles and Cu−O distances, consistent with what has been observed for other transition-metal monodentate aryloxides.[72]

Figure 7 shows an ORTEP of $[Cp_2Co]_2[Co(OAr')_4]$, **10**, in which the anion has no bonding interactions with the cations. The $Co-O_4$ geometry is distorted, having O···O contacts that range from 2.973(7) to 3.286(7) Å (Table 4) and proportionately wider angles for the corresponding O−Co−O angles, 99.3(3)° and 115.4(2)°, respectively.

These distortions are reminiscent of the well-studied D_{2d} $[CoCl_4]^{2-}$ anions.[74] In a CSD survey of 129 $[CoCl_4]^{2-}$ anions (coordination number of cobalt = 4, of each chlorine = 1), the average minimum and maximum Co−Cl distances (Å) were 3.60(9) and 3.82(8) with an average |max − min| value of 0.18(16). The $[Co(OAr')_4]^{2-}$ anion thus exhibits the same distortion seen in $[CoCl_4]^{2-}$.

The cobalt compounds **7a** and **7b**, analogues of **1a** and **1b**, are shown in Figures 8 and S3, respectively. Both cobalt centers have approximately D_{2d} symmetry, like **10** above, rather than T_d, with O−Co−O angles (deg) in the range 97.02(10) to 133.5(2) for **7a** and 96.10(12) to 131.0(2) for **7b**. A T_d geometry was proposed for $(Ph_4P)_2[Co(OAr^F)_4]$.[61] The corresponding minimum and maximum O···O contacts are 2.898(4) to 3.482(4) Å and 2.892(4) to 3.345(4) Å, respectively. In each anion, two $\{K(18\text{-crown-}6)\}^+$ cations weakly bridge the O1···O2 sides of the anion. The distant coordination of the potassium atom to the aryloxide oxygen atoms may be responsible for the slight distortion of **7a** and **7b** from the geometry observed in **10**. The K···O contacts in **7a** and **7b**, listed in Table 4, are long and weak, analogous

(72) Bradley, D. C.; Mehrotra, R. C.; Rothwell, I. P.; Singh, A. In *Alkoxo and Aryloxo Derivatives of Metals*; Academic Press: New York, 2001; Chapter 6, p 671.

(73) Purdy, A. P.; George, C. F.; Brewer, G. A. *Inorg. Chem.* **1992**, *31*, 2633−2638.

(74) Cotton, F. A.; Wilkinson, G.; Murillo, C. A.; Bochmann, M. *Advanced Inorganic Chemistry*; John Wiley & Sons: New York, 1999.

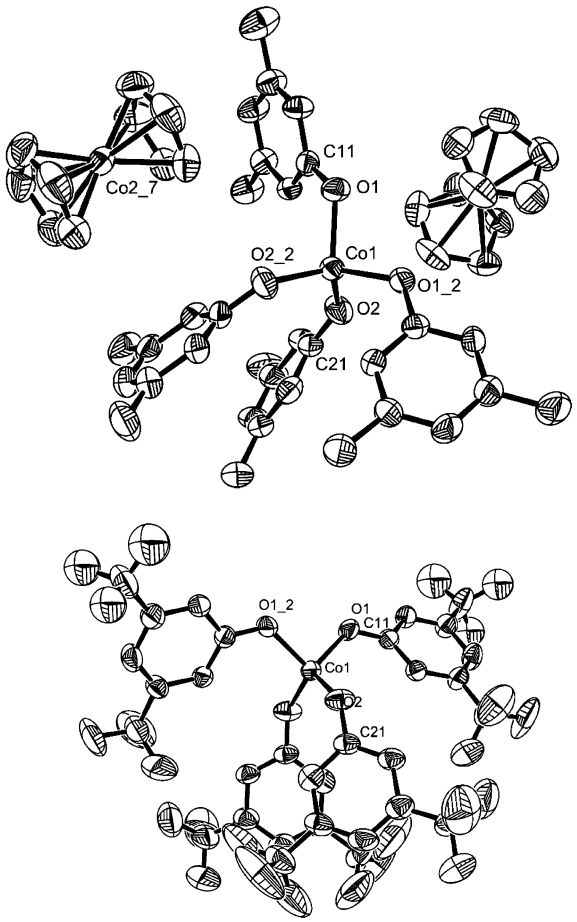

Figure 7. ORTEP diagrams of $[Cp_2Co]_2[Co(OAr')_4]$, **10** (top), with hydrogen and fluorine atoms omitted for clarity and anion of **10** (bottom) with only hydrogen atoms removed. Co(1) sits on a 2-fold rotation axis. Selected distances and angles: Co(1)−O(1) = 1.951(5) Å, Co(1)−O(2) = 1.937(5) Å, O(1)−Co(1)−O(2) = 115.4(2)°. Ellipsoids are shown at the 50% probability level.

to **1a** and **1b**. Like the copper cases described above, the Co−O bonds show no significant lengthening because of potassium interaction, and the $[Co(OAr)_4]^{2-}$ anions contain effectively monodentate phenolates.

Similarly, the $\{Ph_4P\}^+$ cations in **12** do not coordinate to the $[Co(OAr^F)_2Cl_2]^{2-}$ anion and the cobalt center is closest to tetrahedral of **7a**, **7b**, **10**, and **12**, based on the angles (deg) 99.69(9)−117.12(8). The longer Co−Cl versus Co−O bond lengths result in a disparity between O···O and Cl···Cl contact lengths that does not correspond to the narrow range of angles at cobalt. The anion has C_{2v} symmetry because of the two different ligands but is otherwise quite similar to that in the other three pseudotetrahedral cobalt anions.

The range of Co−O distances for monodentate aryloxides in all four structurally characterized fluoroaryloxide cobalt compounds, see Table 4, is narrow. These distances are unexceptional compared to 17 known distances in the CSD for nonbridging, acyclic Co−O(aryl) linkages which average 1.92(7) Å. The Co−O−C angles and O−C distances are unexceptional, and again there is no quantitative or qualitative correlation between Co−O−C angles and Co−O distances for the monodentate ligands.

Table 4. Selected Interatomic Distances, Bond Lengths, and Angles for Cobalt Compounds[a]

compound	distances	(Å)	angles	(deg)
7a	Co1−O1	1.937(2)	O1−Co1−O2	97.02(10)
	Co1−O2	1.932(3)	O1−Co1−O1_1	128.00(15)
	O1···O2	2.898(4)	O2−Co1_O1	108.04(12)
	O1···O1_2	3.482(4)	O2−Co1−O2_1	121.0(2)
	O1···O2_2	3.131(4)	Co1−O1−C1	133.5(2)
	O2···O2_2	3.362(4)	Co1−O2−C7	125.9(2)
	O1−C1	1.310(4)		
	O2−C7	1.305(5)		
	K1−O1	2.784(2)		
	K1−O2	2.811(3)		
7b	Co1−O1	1.947(3)	O1−Co1−O2	96.10(12)
	Co1−O2	1.941(3)	O1−Co1−O1_7	118.29(16)
	O1···O2	2.892(4)	O2−Co1−O1_7	118.69(12)
	O1···O1_7	3.342(4)	O2−Co1−O2_7	110.27(18)
	O1···O2_7	3.345(4)	Co1−O1−C1	131.0(2)
	O2···O2_7	3.186(4)	Co1−O2−C9	128.5(2)
	O1−C1	1.309(4)		
	O2−C9	1.307(5)		
	K1−O1	2.824(3)		
	K1−O2	2.761(3)		
10	Co1−O1	1.951(5)	O1−Co1−O2	115.4(2)
	Co1−O2	1.937(5)	O1−Co1−O1_2	99.3(3)
	O1···O2	3.286(7)	O1−Co1−O2_2	105.7(2)
	O1···O1_5	2.973(7)	O2−Co1−O2_2	114.5(3)
	O1···O2_5	3.099(7)	Co1−O1−C1	125.0(4)
	O2···O2_5	3.260(7)	Co1−O2−C7	135.6(5)
	O1−C1	1.325(8)		
	O2−C7	1.313(9)		
11	Co1−O1	1.962(3)	O1−Co1−O2	117.76(15)
	Co1−O2	1.911(4)	O2−Co1−O3	114.12(16)
	Co1−O3	1.901(3)	O3−Co1−O1_2	104.80(15)
	Co1−O1_2	2.000(3)	O1−Co1−O1_2	80.33(15)
	Co1···Co1_2	3.028(2)	O2−Co1−O1_2	117.75(15)
	O1···O2	3.316(5)	O1−Co1−O3	117.00(16)
	O2···O3	3.199(5)	Co1−O1−Co1_2	99.67(15)
	O1···O3	3.294(5)	Co1−O1−C1	130.6(3)
	O1···O1_2	2.556(5)	Co1−O2−C7	126.1(3)
	O2···O1_2	3.348(5)	Co1−O3−C13	128.6(4)
	O3···O1_2	3.091(5)		
	O1−C1	1.341(6)		
	O2−C7	1.318(6)		
	O3−C13	1.315(6)		
	K1−C10	3.302(6)		
	K1−C15	3.458(7)		
	K1−C16	3.240(6)		
	K1−C17	3.251(7)		
	K1−C18	3.493(5)		
12	Co1−O1	1.962(2)	O1−Co1−O2	99.69(9)
	Co1−O2	1.969(2)	O1−Co1−Cl1	104.28(6)
	Co1−Cl1	2.2782(8)	O1−Co1−Cl2	117.12(8)
	Co1−Cl2	2.2845(8)	O2−Co1−Cl1	114.65(7)
	O1···O2	3.005(3)	O2−Co1−Cl2	109.12(7)
	O1···Cl1	3.353(2)	Cl1−Co1−Cl2	111.62(3)
	O1···Cl2	3.627(2)	Co1−O1−C1	120.66(18)
	O2···Cl1	3.579(2)	Co1−O2−C7	131.30(19)
	O2···Cl2	3.470(2)		
	Cl1···Cl2	3.774(2)		
	O1−C1	1.308(3)		
	O2−C7	1.280(4)		

[a] Numbers in parentheses are estimated deviations of the last significant figure.

The dimeric structure of **11**, Figure 9, like that of **6**, shows the effects of lack of fluorination on the aryloxide binding motif. In **11**, the two cobalt centers each are bridged by two phenoxide ligands and have two monodentate terminal phenoxides. The data in Table 4 show bond lengths longer by ~0.5 Å for the bridging versus the terminal ligands. Again like **6**, the terminal Co−O distances in **11** are shorter than

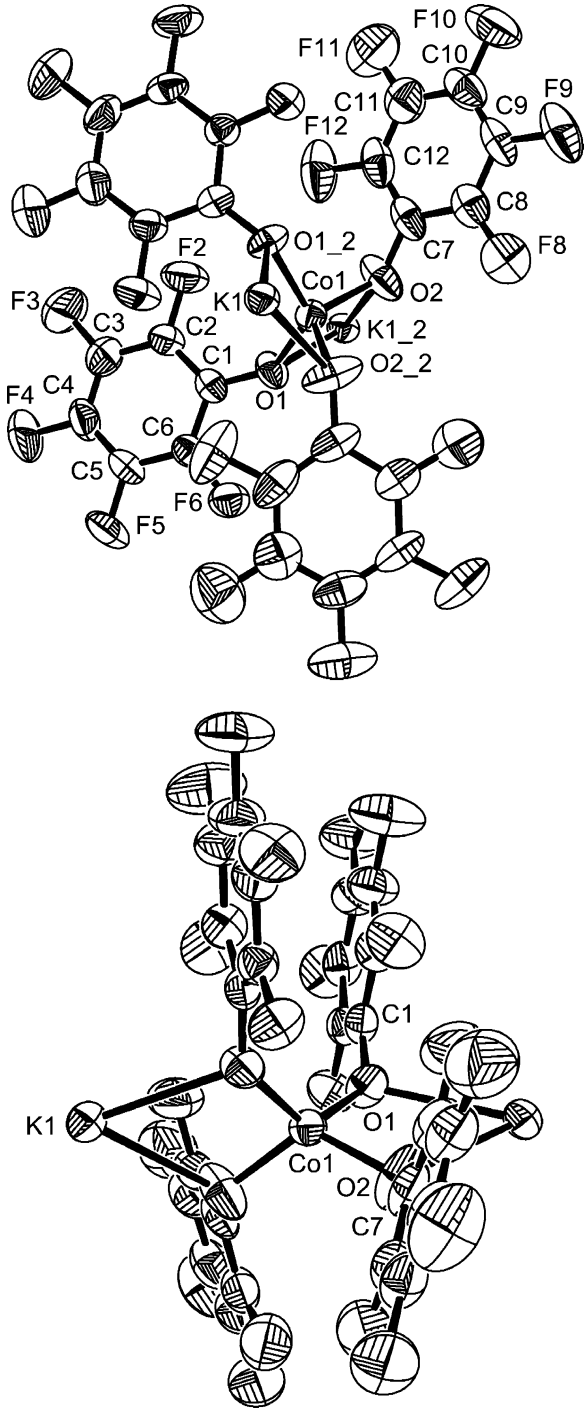

Figure 8. ORTEP diagrams of $\{K(18\text{-crown-6})\}_2[Co(OAr^F)_4]$, **7a**. The cobalt atom sits on a 2-fold rotation axis. Crown ether molecules and one unbound THF molecule in the lattice have been removed for clarity. Selected distances and angles: Co(1)−O(1) = 1.937(2) Å, Co(1)−O(2) = 1.932(3) Å, O(1)−Co(1)−O(2) = 97.02(10)°. Ellipsoids are shown at the 50% probability level.

those in **7a**, **7b**, and **10** because of the greater basicity of the OPh versus fluorinated OAr ligands. The symmetry at the crystallographically equivalent cobalt centers is C_{2v} because the O1···O1_3 contact (Å) is 2.556(5) compared to 3.199(5) between O2 and O3, and the subtended angles (deg) are 80.33(15) and 114.12(16), respectively. The most interesting structural feature is the virtual coplanarity of both bridging phenoxides and the Co_2O_2 core. In the copper

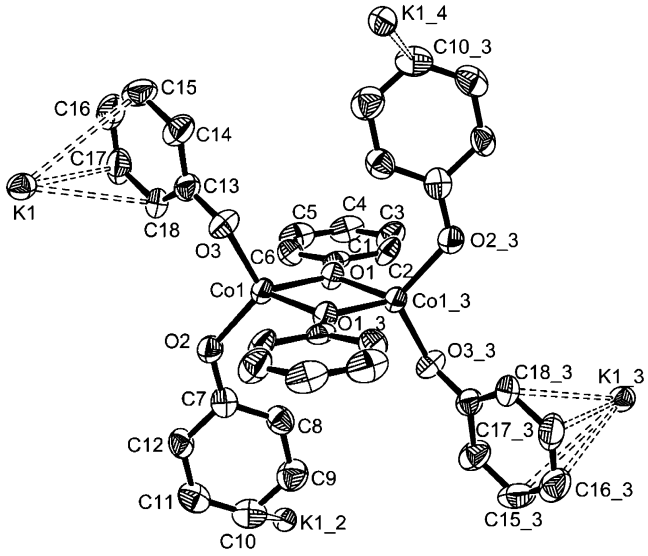

Figure 9. ORTEP diagram of $\{K(18\text{-crown-6})\}_2[Co_2(\mu\text{-OPh})_2(OPh)_4]$, **11**. The two cobalt atoms are related by a center of inversion. Crown ether molecules, hydrogen atoms, and one molecule of lattice CH_2Cl_2 have been omitted for clarity. Selected distances and angles: Co(1)−O(1) = 1.962(3) Å, Co(1)−O(2) = 1.911(4) Å, Co(1)−O(3) = 1.901(3) Å, Co(1)···Co(1_3) = 3.028(2) Å, Co(1)−O(1)−Co(1_3) = 99.67(15)°. Ellipsoids are shown at the 50% probability level.

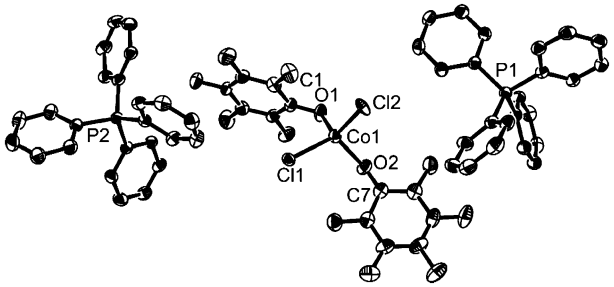

Figure 10. ORTEP diagram of $(Ph_4P)_2[CoCl_2(OAr^F)_2]$, **12**. Hydrogen atoms have been omitted for clarity. Selected distances and angles: Co(1)−O(1) = 1.962(2) Å, Co(1)−O(2) = 1.969(2) Å, Co(1)−Cl(1) = 2.2782(5) Å, Co(1)−Cl(2) = 2.2845(8) Å, O(1)−Co(1)-O(2) = 99.69(9)°, Cl(1)−Co(1)−Cl(2) = 111.62(3)°. Ellipsoids are shown at the 50% probability level.

analogue **6**, the phenoxide rings are perpendicular to the Cu_2O_2 core. The dihedral angle between the C2−C1−C6 plane and the Co1−O1−Co1_3 plane is only 5.57°. Only two other structures with bridging but nonchelating phenoxides have been crystallographically characterized, one with Klaui ligands and pentacoordinate cobalt atoms[75] and one with distorted tetrahedral cobalt centers, $(Et_4N)_2[Co_2Cl_4(\mu\text{-}4\text{-}OC_6H_4CH_3)_2]$.[76,77] In the latter, the analogous dihedral angle is 8.3°. In most aspects, the dinuclear compound **11** has a similar structure to **6** except that the cobalt atoms are approximately tetrahedral with a dihedral angle at cobalt of 84.11°. There are no close contacts between the $\{K(18\text{-crown-6})\}^+$ cations and the phenolate oxygen atoms, however. One axial site of the potassium is coordinated by

(75) Ma, D.-q.; Hikichi, S.; Akita, M.; Moro-oka, Y. *Dalton* **2000**, 1123−1134.
(76) Coucouvanis, D.; Greiwe, K.; Salifoglou, A.; Challen, P.; Simopoulos, A.; Kostikas, A. *Inorg. Chem.* **1988**, *27*, 593−594.
(77) Emori, S.; Nakashima, M.; Mori, W. *Bull. Chem. Soc. Jpn.* **2000**, *73*, 81−84.

an η^4-phenoxide (C15−C18) and the antipodal site is occupied by an η^1-phenoxide (C10). The K−C distances (Å) listed in Table 4 are consistent with 182 similar contacts in the CSD, having an average distance of 3.25(16) and the range 2.90−3.93.

Information on the solution structure of some of these compounds was obtained from conductivity studies. The conductivities of six CH_2Cl_2 solutions each of **12**, $(Ph_4P)_2[CoCl_2(OAr^F)_2]$, and **8a**, $[Tl_2(Co(OAr^F)_4]$, were measured at varying concentrations. The conductivity of **8a** is insensitive to changes in concentration, demonstrating that the thallium cations are covalently bound to the phenolate anion. In contrast, the conductivity of solutions of **12** increases linearly with the increases in concentration, demonstrating separated cations and anions. Data are plotted in Figure S4.

IR spectra are not particularly informative as they are dominated by strong absorptions for C═C stretches from the aryloxide rings. Spectra for compounds **3**, **6**, **9**, and **11** are presented in Figure S5. In the region of ν(C−O)M bands (900−1150 cm^{-1}), all four complexes exhibit a very weak absorption around 1110 cm^{-1}. The mononuclear compounds (**3** and **9**) exhibit slightly stronger stretches at 972 and 1007 and 988 and 1011 cm^{-1}, respectively whereas the dinuclear species (**6** and **11**) exhibit weak bands at 1585 and 1583 cm^{-1}, respectively. M−O bands for first row metals typically are below 600 cm^{-1}.[24]

Electronic Structure. The $[CuCl_4]^{2-}$ anion is well-studied and provides an initial model for discussion of the $[Cu(OAr)_4]^{2-}$ anions described here. Early crystallographic work[78] established a wide range of geometries from distorted tetrahedral (D_{2d}) to square planar (D_{4h}) for $[CuCl_4]^{2-}$. The anion is also found in bridged forms such as $[Cu_2Cl_6]^{2-}$, $[Cu_4Cl_{10}]^{2-}$, $[Cu_4Cl_{12}]^{4-}$, and $[Cu_5Cl_{14}]^{4-}$, making spectroscopic "signatures" inadequate proof of discrete $[CuX_4]^{2-}$ anions. The $[Cu(OAr)_4]^{2-}$ compounds reported herein are in distinct contrast because they can be routinely prepared as monomeric units, and thus detailed studies of their electronic and magnetic properties were undertaken. In a recent CSD search, 217 structures were found with coordinates for an isolated $[CuCl_4]^{2-}$ anion (each chlorine coordination number = 1), and only 36 of them have maximum Cl−Cu−Cl angles of greater than 175°, thus square planar anions are less common but not infrequent. Among these anions, 21 have a standard deviation in the short Cl···Cl distances of more than 0.01 Å, indicative of symmetry reduction to D_{2h} geometry.

Our crystallographic work (vide supra) has shown that the $[Cu(OAr)_4]^{2-}$ anions are planar with a slight distortion from D_{4h} to D_{2h} symmetry. We base our spectroscopic assignments on D_{4h} symmetry because this distortion is not very large. Work by Solomon and others[79,80] on square planar $[CuCl_4]^{2-}$ has demonstrated that in the ground state the d-orbital manifold in D_{4h} symmetry has decreasing energies as

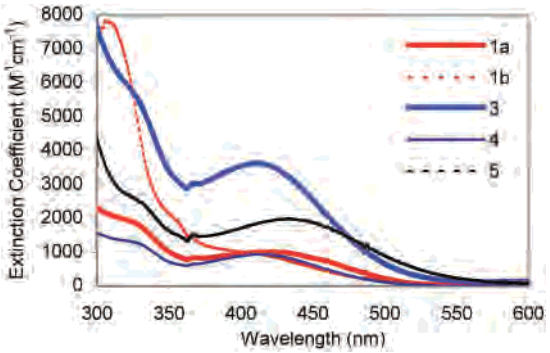

Figure 11. Visible spectra of $[Cu(OAr)_4]^{2-}$ complexes $\{K(18\text{-crown-}6)\}_2[Cu(OAr^F)_4]$, **1a**, $\{K(18\text{-crown-}6)\}_2[Cu(OAr')_4]$, **1b**, $(Ph_4P)_2[Cu(OAr^F)_4]$, **3**, $(^nBu_4N)_2[Cu(OAr^F)_4]$, **4**, and $(HEt_3N)_2[Cu(OAr^F)_4]$, **5**.

$B_{1g}(d_{x^2-y^2}) \gg B_{2g}(d_{xy}) > E_g(d_{xz}, d_{yz}) > A_{1g}(d_{z^2})$. The solid samples of **1a**, **1b**, **3**, **4**, and **5** are bright green and retain the color in THF or CH_2Cl_2 solutions. The visible spectra for **1a**, **1b**, **3**, **4,** and **5** are compared in Figure 11. For comparison, the visible spectrum of $(^nBu_4N)_2[CuCl_4]$ has absorptions at 340, 400, and 450 nm.[78] All the complexes with $[Cu(OAr^F)_4]^{2-}$ anions have strong absorbances in the UV region, suggesting that some ligand-to-metal charge-transfer bands overlap with intraligand $\pi-\pi^*$ transitions. On the low energy side of these broad absorbances, there are shoulders near 330 nm that we assign as $B_{1g} \leftarrow E_g$ transitions and broad maxima near 425 nm that are assigned as $B_{1g} \leftarrow B_{2g}$ transitions. The lowest energy transition of all the phenolate complexes is blue-shifted compared to that of the $[CuCl_4]^{2-}$ species, consistent with larger splitting parameters for oxygen donor atoms versus chlorine. The effect of different cations on λ_{max} is minimal with absorptions for **3** and **4** at 411 and 414 nm, respectively. The spectrum of **5** with $\{Et_3NH\}^+$ cations has a λ_{max} value shifted slightly to 432 nm. The $[Cu(OAr')_4]^{2-}$ spectrum in **1b** differs from the other four, which all contain OAr^F, in the absence of distinct maxima near 330 or 420 nm but a maximum at 308 nm that is relatively sharp. Further differences between $[M(OAr^F)_4]^{2-}$ and $[M(OAr')_4]^{2-}$ spectra are discussed below.

Similarly we reference our discussion of the $[Co(OAr)_4]^{2-}$ electronic structure to the literature on $[CoCl_4]^{2-}$ anion. Extensive structural work has determined a flattened-tetrahedron D_{2d} structure for $[CoCl_4]^{2-}$ anions. In the same CSD search quoted above (129 hits), the average maximum Cl−Co−Cl angle is 133(4)°. The electronic spectra have been described in terms of a tetrahedral ligand field,[81] despite this noticeable distortion. Absorptions in UV−vis spectra of $[CoX_4]^{2-}$ anions have been assigned to three band groups ν_1 ($^4T_2 \leftarrow {}^4A_2$ far UV), ν_2 ($^4T_1(F) \leftarrow {}^4A_2$, approximately 425−830 nm), and ν_3 ($^4T_1(P) \leftarrow {}^4A_2$, approximately 1430−2220 nm).[82]

In our compounds with $[Co(OAr)_4]^{2-}$ anions, there is no O−Co−O angle greater than 128°, and most angles are less than 120°, having approximately tetrahedral structures so we

(78) Smith, D. W. *Coord. Chem. Rev.* **1976**, *21*, 93−158.
(79) McDonald, R. G.; Hitchman, M. A. *Inorg. Chem.* **1986**, *25*, 3273−81.
(80) Desjardins, S. R.; Penfield, K. W.; Cohen, S. L.; Musselman, R. L.; Solomon, E. I. *J. Am. Chem. Soc.* **1983**, *105*, 4590−4603.
(81) Cotton, F. A.; Goodgame, D. M. L.; Goodgame, M. *J. Am. Chem. Soc.* **1961**, *83*, 4690−4699.
(82) Cotton, F. A.; Goodgame, M. *J. Am. Chem. Soc.* **1961**, *83*, 1777−1780.

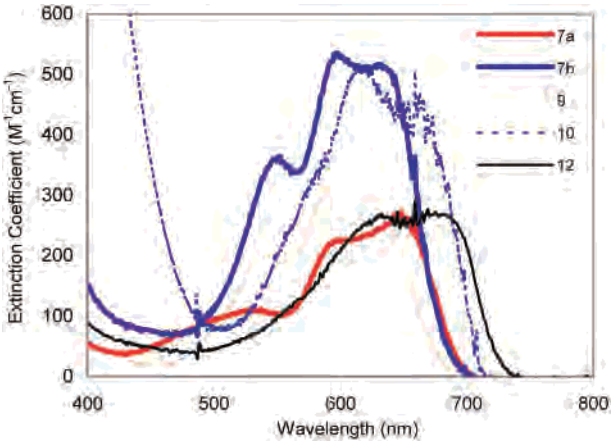

Figure 12. Visible spectra of $[CoX_2(OAr)_2]^{2-}$ complexes {K(18-crown-6)}$_2$[Co(OAr^F)$_4$], **7a**, {K(18-crown-6)}$_2$[Co(OAr′)$_4$], **7b**, $(Me_4N)_2$[Co(OAr^F)$_4$], **9**, $[Cp_2Co]_2$[Co(OAr′)$_4$], **10**, and $(Ph_4P)_2$[Co(OAr^F)$_2$Cl$_2$], **12**.

also assign the spectra based on T_d symmetry. A comparison of the visible spectra of **7a**, **7b**, **9**, **10,** and **12** in THF is presented in Figure 12. We assign these visible transitions to the ν_2 manifold of $^4T_1(F) \leftarrow {}^4A_2$ transitions. The $[CoCl_4]^{2-}$ anion in $(^nBu_4N)_2[CoCl_4]$ exhibits three maxima at λ_{max} (ϵ) = 634 (450), 667 (630), and 699 nm (750 M^{-1} cm^{-1}).[81] The phenolate spectra for **7a**, **7b**, and **9** in Figure 12 also show three maxima in approximately the same region and the magnitudes of the extinction coefficients for all five complexes are consistent with d−d transitions. The strong, broad absorbance less than 400 nm in **10** is due to the thoroughly studied yellow $[Cp_2Co]^+$ cations. The presence of both the yellow cobalticenium cations and blue cobaltate anions accounts for the observed blue-green color of the crystalline complex **10** and its solutions.

The spectra in Figure 12 qualitatively fall into three groups, those with only OAr^F ligands (**7a** and **9**, in red), those with only OAr′ ligands (**7b** and **10**, in blue), and a mixed OAr^F−Cl derivative **12** (in black). Interestingly, the extinction coefficients for **7b** and **10** are greater by almost a factor of 2 versus **7a**, **9**, and **12**. This observation together with the comments about **1b** above suggests that the d−d transitions are more allowed (greater ϵ values) with the OAr′ ligand than with OAr^F.

The spectrum for the less symmetrical $[CoCl_2(OAr^F)_2]^{2-}$ anion in **12** shows two not three maxima, as does the spectrum of **10**. The anion in **12** has C_{2v} symmetry in which the T_1 state is expected to split into A_2, B_1, and B_2 terms, but other C_{2v} $[CoX_2Y_2]^{2-}$ anions have spectra not substantially different from their $[CoX_4]^{2-}$ cousins.[83] The larger λ_{max} at 674 nm for **12** compared to the $[Co(OAr)_4]^{2-}$ containing species is consistent with smaller splitting parameters expected for Cl donor atoms compared to oxygen donor atoms. Similarly, all the absorbances in Figure 12 are blue-shifted relative to those of $[CoCl_4]^{2-}$, consistent with the comparison of the spectra in Figure 11 and that of the $[CuCl_4]^{2-}$ anion. The UV−vis spectra of many [M(catecholate)$_2$]$^{2-}$ complexes have been reported,[84] and those of the Co(II) and Cu(II) species are broadly similar to the spectra reported herein for $[M(OAr)_4]^{2-}$ anions. To date, no structural data for bis-catecholate complexes [M(catecholate)$_2$]$^{2-}$ have been reported.

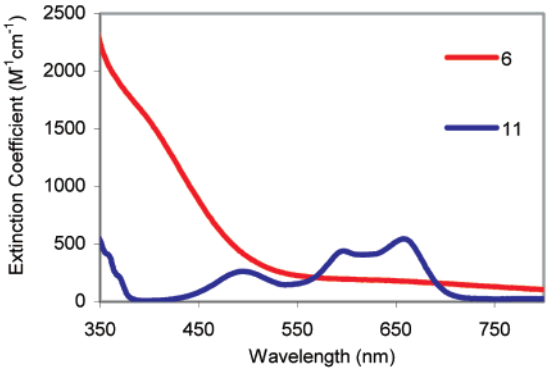

Figure 13. Visible spectra of $[M_2(\mu\text{-OPh})_2(OPh)_4]^{2-}$ compounds {K(18-crown-6)}$_2$[Cu$_2$(μ_2-OC$_6$H$_5$)$_2$(OC$_6$H$_5$)$_4$], **6**, and {K(18-crown-6)}$_2$[Co$_2$(μ_2-OC$_6$H$_5$)$_2$(OC$_6$H$_5$)$_4$], **11**.

Table 5. Summary of Magnetic Moment Data

compound	compound formulation	μ_{eff} (μ_B)
1a	{K(18-crown-6)}$_2$[Cu(OAr^F)$_4$]	1.74
1b	{K(18-crown-6)}$_2$[Cu(OAr′)$_4$]	1.79
2a	Tl$_2$[Cu(OAr^F)$_4$]	1.79
2b	Tl$_2$[Cu(OAr′)$_4$]	1.94
3	$(Ph_4P)_2$[Cu(OAr^F)$_4$]	1.59
4	$(^nBu_4N)_2$[Cu(OAr^F)$_4$]	1.87
5	$(HEt_3N)_2$[Cu(OAr^F)$_4$]	1.72
6	{K(18-crown-6)}$_2$[Cu$_2$(OPh)$_6$]	2.74
7a	{K(18-crown-6)}$_2$[Co(OAr^F)$_4$]	4.53
7b	{K(18-crown-6)}$_2$[Co(OAr′)$_4$]	5.02
8a	[Tl$_2$Co(OAr^F)$_4$]	4.46
8b	{Tl$_2$[Co(OAr′)$_4$]·toluene}$_2$	6.06
9	$(Me_4N)_2$[Co(OAr^F)$_4$]	4.56
10	$[Cp_2Co]_2$[Co(OAr′)$_4$]	4.67
11	{K(18-crown-6)}$_2$[Co$_2$(OPh)$_6$]	5.68
12	$(Ph_4P)_2$[Co(OAr^F)$_2$Cl$_2$]	4.45

The visible-region electronic spectra of the two dinuclear $[M_2(\mu\text{-OPh})_2(OPh)_4]^{2-}$ compounds are shown in Figure 13. The copper complex **6** is brown in solution and the solid state, in contrast to the green mononuclear derivatives, and shows no clear maxima in the visible region but a broad shoulder around 390 nm. The dinuclear cobalt derivative **11** is bright blue as a solid and in solution and shows correspondingly blue-shifted absorbances compared to those of the dark cobalt-blue mononuclear compounds. There are three maxima at 496, 598, and 659 nm for the formally C_{2v} metal centers, but the general pattern matches those of the more tetrahedral CoO_4 centers described above.

Magnetism. Solution measurements of magnetically dilute samples by the Evans' method[36,37] yielded the magnetic susceptibilities listed in Table 5. The compounds **1**−**5** that contain $[Cu(OAr)_4]^{2-}$ anions have moments > 1.73μ_B (spin-only moment for one unpaired electron) and in the range 1.74−1.94μ_B. Magnetic susceptibilities for compounds with $[CuCl_4]^{2-}$ anions are ~1.90μ_B,[78] with quenching expected of the orbital angular momentum in D_{4h} symmetry (no T states).[85] Dimeric **6** has a significantly larger value at 2.74μ_B (1.37μ_B /Cu) that indicates some coupling between the two

(83) Cotton, F. A.; Goodgame, D. M. L.; Goodgame, M.; Sacco, A. *J. Am. Chem. Soc.* **1961**, *83*, 4157−4161.

(84) Sever, M. J.; Wilker, J. J. *Dalton Trans.* **2004**, 1061−1072.

copper centers.[39] Detailed magnetic studies of **6** and **11** and other polynuclear phenolates (**2a**, **2b**, and **8b**) will be reported in a future publication.

The $[Co(OAr)_4]^{2-}$ family of anions show values that are noticeably higher than the spin-only value of $3.87\mu_B$ for three unpaired electrons, namely, in the range $4.45-5.02\mu_B$, and such behavior has been observed previously for several $[CoX_4]^{2-}$ compounds.[81−83,86,87] The susceptibility of **8b** is noticeably higher than that of the other compounds, but as previously mentioned the single-crystal X-ray diffraction studies of the $[Tl_2M(OAr)_4]$ family reveal them to contain aryloxide ligands that bridge the Tl^+ and M^{2+} metal centers or two M^{2+} centers. This large magnetic susceptibility in solution suggests that a structure with bridging aryloxide ligands and coupling between cobalt centers persists in solution.

The magnetic susceptibility of dinuclear **11**, like that of **6**, suggests a coupling interaction between the cobalt centers. Two related anions $[Cl_2Co_2(\mu_2\text{-}OPh)_2Cl_2]^{2-}$ and $[Cl_2Co_2(\mu_2\text{-}O\text{-}p\text{-}tolyl)_2Cl_2]^{2-}$ have been characterized in the solid state both structurally[76,77] and magnetically.[77] The latter studies show small antiferromagnetic interactions in the solid state, consistent with the solution susceptibilities reported herein. Both compounds with bridging phenoxide ligands, **6** and **11**, show higher susceptibilities than either predicted spin-only moments for mononuclear compounds or the values observed for the magnetically isolated mononuclear compounds.

Electrochemistry. The four transition metal complexes $\{K(18\text{-crown-}6)\}_2[Cu(OAr^F)_4]$, **1a**, $\{K(18\text{-crown-}6)\}_2[Cu(OAr')_4]$, **1b**, $\{K(18\text{-crown-}6)\}_2[Co(OAr^F)_4]$, **7a**, and $\{K(18\text{-crown-}6)\}_2[Co(OAr')_4]$, **7b**, were studied by cyclic voltammetry as were the related compounds $[K\{18\text{-crown-}6\}(OAr^F)]$ and $[K\{18\text{-crown-}6\}(OAr')]$. Control studies of the two potassium phenolates indicated that both ligands show no reversible or irreversible reduction features within the solvent window to −2.5 V (versus Ag). Under oxidation, the ligands are similarly stable out to +2.0 V (versus Ag). Beyond this point, both phenoxides show chemically irreversible oxidation consistent with formation of a phenoxyl radical, which undergoes followup chemistry. The behavior of the pentafluorophenoxyl radical in aqueous solution has been studied.[88]

The Cu species show irreversible oxidations at potentials near 2.50 V with $[Cu(OAr')_4]^{2-}$ and 2.0 V for $[Cu(OAr^F)_4]^{2-}$ versus Ag. In the former case the parent material appears to show surface activity (peak current proportional to scan rate), suggesting the adsorption of the Cu(OAr′) ion/ion pair, whereas the latter shows diffusional behavior (peak current proportional to square root of scan rate). In both cases, the oxidative potentials are close to those of the ligands and suggest that the oxidation removes electrons from the phenolate group and not from the metal center. No reduction voltammetry was observed. Turning to the Co species, similar observations were made; no reduction voltammetry and oxidative waves correspond to ligand electrolysis. The only point of difference being that for $[Co(OAr')_4]^{2-}$ the wave was diffusional as observed for the related copper compound **1b**. Although the Co and Cu species show no reversible electrochemical oxidation or reduction behavior, which would suggest possible formation of formally $[M^{III}(OAr)_4]^-$ or $[M^{I}(OAr)_4]^{3-}$ species, preliminary chemical studies have shown that the Cu^{2+} can be oxidized by strong oxidants such as Ce^{4+} and O_2.[89] Representative cyclic voltammograms for all six compounds are provided in the Supporting Information, Figures S6−S11.

Conclusions

The syntheses of two families of late transition metal homoleptic phenolate anions with fluorinated aryloxides of the form $[M(OAr)_4]^{2-}$ are reported with thorough spectroscopic and structural characterization. By use of fluorinated aryloxide ligands, the electron density on the ligating oxygen atoms seems to be sufficiently reduced so that bridging between transition-metal centers can be prevented. Reactions with OPh under the same conditions led to dimeric anions of the form $[M_2(\mu_2\text{-}OC_6H_5)_2(OC_6H_5)_4]^{2-}$. The compounds herein provide several examples of monodentate aryloxide coordination without the use of chelating or cyclic ligands. The structural comparisons between the copper anions in $[Cu(OAr^F)_4]^{2-}$ and $[Cu_2(\mu_2\text{-}OC_6H_5)_2(OC_6H_5)_4]^{2-}$ and between the cobalt anions in $[Co(OAr^F)_4]^{2-}$ and $[Co_2(\mu_2\text{-}OC_6H_5)_2(OC_6H_5)_4]^{2-}$ demonstrate that by changing the electronegativity of the ligand the degree of oligomerization can be affected. After decades of research in metal−aryloxide chemistry and struggles with bridging ligands, the structures of these seemingly simple $[M(OAr)_4]^{2-}$ anions are only now being reported for the first time.

An exciting target for these systems is the chemistry of higher oxidation states that we are actively pursuing at this time. Oxygen atoms are often the ligand of choice for stabilizing high oxidation states (e.g., $[OsO_4]$, $[MnO_4]^-$) and oxygen-donor ligands can also serve in this capacity. The organic moieties attached to oxygen can often be attacked intra- or intermolecularly by the resultant high oxidation state, and a great deal of work has gone into control or prevention of such C−H activation.[90] Fluorination of the aryloxide rings not only makes them resistant to C−H activation and subsequent decomposition but increases their electron-withdrawing capacity. These readily accessible $[M(OAr)_4]^{2-}$ units open the door to a plethora of new compounds as well as electronic structure and reactivity studies that were previously unavailable.

Acknowledgment. This work was supported by startup funds from Barnard College, a Camille and Henry Dreyfus Faculty Startup Grant (SU-99-065), a Research Corporation

(85) Figgis, B. N.; Hitchman, M. A. *Ligand Field Theory and its Applications*; Wiley-VCH: New York, 2000.
(86) Holm, R. H.; Cotton, F. A. *J. Chem. Phys.* **1959**, *31*, 788−792.
(87) Holm, R. H.; Cotton, F. A. *J. Chem. Phys.* **1960**, *32*, 1168−1172.
(88) Shoute, L. C. T.; Mittal, J. P.; Neta, P. *J. Phys. Chem.* **1996**, *100*, 3016−19.
(89) Iqbal, A.; Saddoughi, S.; Turner, J. F. C.; Doerrer, L. H. Unpublished results.
(90) Collins, T. J. *Acc. Chem. Res.* **1994**, *27*, 279−285.

CCSA Award (CC5398), an NSF-CAREER award (to L.H.D.; CHE-0134817), and the 2000 Moissan Undergraduate Research Fellowship in Chemistry from the Fluorine Division of the ACS to M.C.B.. The Barnard College NMR facility is supported by the National Science Foundation (DUE-9952633). L.H.D. thanks C. C. Cummins for hospitality during a sabbatical when some of these data were collected on the MIT DCIF NMR spectrometer funded through NSF Grant CHE-9808061. We thank J. R. Norton for the loan of a YSI Conductivity Bridge. We also thank G. Parkin and D. Churchill for collecting the raw X-ray data for **1a**, **1b,** and **10** and thank L. N. Zakharov for data collection and structure solution for **2a**, **2b, 4**, **5**, **7a**−**8b**, and **12**, modeling the CF_3 disorders in **1b** and **10**, all CIF file preparations, and thoughtful discussions.

Supporting Information Available: ^{1}H NMR data for the preparation of **10**, structures **4** and **7b**, the conductivity data, IR spectra, cyclic voltammograms, and X-ray crystallographic data in CIF format. This material is available free of charge at http://pubs.acs.org.

IC0493954